Published in final edited form as:

Leukemia. 2016 March ; 30(3): 580–593. doi:10.1038/leu.2015.140.

Differential PAX5 levels promote malignant B cell infiltration, progression and drug resistance and predict a poor prognosis in MCL patients independent of CCND1

Albert E. Teo[1], **Zheng Chen**[1], **Roberto N. Miranda**[2], **Timothy McDonnell**[2], **L. Jeffrey Medeiros**[2], and **Nami McCarty**[1,*]

[1]Center for Stem Cell and Regenerative Disease, Brown Foundation Institute of Molecular Medicine for the Prevention of Human Diseases (IMM), The University of Texas-Health Science Center at Houston, Houston, Texas, 77030, USA

[2]Department of Hematopathology, The University of Texas MD Anderson Cancer Center, Houston, Texas, 77030, USA

Abstract

Reduced PAX5 levels play important roles in the pathogenesis of human B-cell acute lymphoblastic leukemia. However, the role of PAX5 in human lymphoma remains unclear. We generated PAX5-silenced cells using mantle cell lymphoma (MCL) as a model system. These PAX5^{-} MCL cells exhibited unexpected phenotypes, including increased proliferation in vitro, enhanced tumor infiltration in vivo, robust adhesion to bone marrow stromal cells, and increased retention of quiescent stem-like cells. These phenotypes were attributed to alterations in the expression of genes including p53 and Rb and to PI3 kinase/mTOR and pSTAT3 pathway hyperactivation. Upon PAX5 silencing, the MCL cells displayed upregulated IL-6 expression and increased responses to paracrine IL-6. Moreover, decreased PAX5 levels in CD19+ MCL cells correlated with their increased infiltration and progression; thus, PAX5 levels can be used as a prognostic marker independent of cyclin D1 in advanced MCL patients. Importantly, high-throughput screening of 3800 chemical compounds revealed that PAX5−MCL cells are highly drug-resistant compared to PAX5 wild-type MCL cells. Collectively, the results of our study support a paradigm shift regarding the functions of PAX5 in human B cell cancer and encourage future efforts to design effective therapies against MCL.

INTRODUCTION

The transcription factor Paired box 5 (Pax5) plays a central role in restricting the differentiation of lymphoid progenitors toward the B cell lineage.[1] Similar to other PAX family members, Pax5 contains a conserved ‘paired’ domain, which functions as a bipartite DNA-binding region consisting of N- and C-terminal sub-domains.[2] This bipartite domain

*Contact: Nami McCarty, The University of Texas-Health Science Center at Houston, 1835 Pressler St., IMM-630H, Houston, TX 77030, USA. ; Email: nami.mccarty@uth.tmc.edu Tel: 713-500-2495, Fax: 713-500-2424

Authors have no conflicts of interest.

interacts with degenerate Pax5 consensus binding sites, and multiple sequence variants can increase the affinity of one half-site while decreasing the affinity of other half-site.[3] By the pro-B cell stage, Pax5 is uniformly expressed until it becomes downregulated during plasma cell differentiation.[4,5] During this physiological downregulation, many Pax5-repressed genes are re-expressed, and B cell-specific gene expression is altered.[6, 7] Pax5-deficient ($Pax5^{-/-}$) pro-B cells can differentiate into functional macrophages, granulocytes, dendritic cells, osteoclasts or natural killer cells in vivo.[7,8] In addition, $Pax5^{-/-}$ pro-B cells differentiate in vitro into functional T cells in the presence of OP9 stromal cells expressing the Notch ligand Delta-like 1.[9]

Despite its established role as a determinant of normal B cell lineage commitment, the role of PAX5 in the development and progression of human B cell cancer is controversial. For example, PAX5 has been implicated in certain lymphomas as an oncogene via a gain-of-function mutation.[10] In contrast, human B-progenitor acute lymphoblastic leukemia harbors monoallelic mutations that reduce PAX5 protein expression.[11] Ablating Pax5 gene expression in mice leads to spontaneous B cell malignancies,[12] a finding that supports a role of PAX5 as a potential tumor suppressor. Hence, the exact role of PAX5 in human lymphoma initiation and progression remains enigmatic.

To directly address this controversial issue, we silenced PAX5 expression in MCL cells using lentivirus. MCL accounts for approximately 6% of all Non-Hodgkin's Lymphomas (NHLs), and most tumors become highly refractory to standard radiation and chemotherapy, contributing to one of the worst survival rates among NHL patients. [13] A major genomic abnormality in MCL, which also distinguishes them from low-grade B cell lymphoma cases, is the t(11;14)(q13;q32) translocation, which leads to increased cyclin D1 (CCND1) expression due to the juxtaposition of CCND1 with B cell IgG heavy chain transcriptional enhancers.[14] However, transgenic mice overexpressing CCND1 in B cells do not develop spontaneous lymphoma, revealing that CCND1 overexpression alone is not sufficient to induce MCL and that alternative genetic or epigenetic mechanisms are required [15, 16].

Interestingly, silencing PAX5 in MCL resulted in unexpected phenotypes, including increased cell proliferation in vitro, increased tumor infiltration in vivo, increased cell adhesion to bone marrow stromal cells (BMSCs) and increased retention of quiescent stem-like cells, suggesting that decreased PAX5 levels promote tumor progression. Importantly, the PAX5 levels were associated with the clinical outcomes of MCL and drug resistance.

Collectively, our data define novel functions of PAX5 in human MCL, as PAX5 downregulation conferred increased cell proliferation and led to the overexpression of specific prosurvival pathways that contribute to MCL progression and increased tumor infiltration. Our findings support a paradigm shift regarding the functions of PAX5 in human B cell lymphoma.

METHODS

Cell lines

The human MCL cell lines SP53 and Jeko were obtained from the American Type Culture Collection (Manassas, VA). HS5 BMSCs were a kind gift from Dr. B. Torok-Storb (Fred Hutchinson Cancer Research Center, Seattle, WA). Cells were maintained under standard conditions (5% CO_2, 37°C).

Human MCL samples

Blood or bone marrow specimens from MCL patients were obtained after receiving informed consent, as approved by the MD Anderson Cancer Center (MDACC) and the University of Texas-Health Science Center Institutional Review Boards.

Adhesion assay

HS5 human BMSCs were seeded in a 24-well plate and allowed to form a monolayer over 48–72 hrs. MCL cell lines were stained with the membrane dye PKH26 (Sigma, St. Louis, MO) according to the manufacturer's protocol. The cells (5×10^5) were then plated on the pre-established monolayer of HS5 cells and allowed to adhere for 1 hour at 37°C. After washing twice with 1 × PBS, the PKH26 dye intensity was measured using an Infinite®M1000 fluorescence plate reader (TECAN, Morrisville, NC). Wells containing only MCL cells that were not subjected to a wash step served as 100% adhesion controls, and wells containing only the monolayer of HS5 cells served as 0% adhesion controls.

Other methods are described in the Supplemental Methods.

RESULTS

PAX5 silencing increases MCL cell proliferation, and PAX5 overexpression induces MCL cell death

We generated two cell lines in which PAX5 was stably knocked down: $PAX5^-$ Jeko and $PAX5^-$ SP53 MCL cells. Lentiviral PAX5 shRNA transduction efficiently silenced PAX5 expression in GFP+ SP53 and Jeko cells (Supplementary Figure 1a), whereas PAX5 ORF lentiviral infection generated PAX5-overexpressing cells (Supplementary Figure 1b). We next compared the proliferation of $PAX5^-$ MCL cells to that of control cells transfected with scrambled RNA. Unexpectedly, cell proliferation was significantly increased in $PAX5^-$ MCL cells (Figure 1a). In contrast, PAX5 overexpression ($PAX5^{ORF}$) severely reduced cell proliferation (Figure 1b) and increased apoptosis in these cells (Supplementary Figure 1c). $PAX5^-$ MCL cells also thrived under serum-starved conditions; $PAX5^-$ MCL cells exhibited significantly increased cell survival in 2% or 5% serum (Figure 1b; Supplementary Figure 1d), indicating that silencing PAX5 promotes MCL cell survival not only under normal cell culture conditions but also under stressed conditions.

Cell cycle regulator expression is altered in $PAX5^-$ MCL cells

MCL cells included approximately 50–60% more cells in S phase and 30–40% fewer cells in G0/G1 phase than control cells (Supplementary Figure 1e). Cyclin-dependent kinase (CDK)

deregulation has been linked to increased cellular proliferation and genomic and chromosomal instability, and these alterations can contribute to tumor progression.[17_19] PAX5$^-$ MCL cells demonstrated increased levels of cyclin genes involved in G1 progression, such as CCNE1 and CCNA2 (Figure 1c), and of corresponding G1 phase-related CDKs, including CDK2, CDK6 (Figure 1c) and CDK4 (Figure 1d). The deregulation of the gene and protein expression of the tumor suppressors TP53, RB and CDKN1A (p21) leads to lymphoma development.[20,21] SP53 cells, which harbor wild-type p53,[22,23] expressed decreased TP53, CDKN1A and CDKN1B levels upon PAX5 silencing (Figure 1d and e). These alterations collectively resulted in increased MCL cell proliferation.

Approximately 110 genes are normally repressed by Pax5 in murine B cells [6,24] We selected 13 genes that had previously been reported to be involved in cancer development or hematopoietic stem cell (HSC) function (Supplementary Table 1). Among these 13 Pax5-repressed genes, 10 genes were significantly upregulated in PAX5$^-$ SP53 cells (Supplementary Figure 2), and 7 were significantly upregulated in PAX5$^-$ Jeko cells (Supplementary Figure 2). These data suggest that PAX5 may control a gene profile contributing to uncontrolled MCL cell proliferation that is similar between human and mouse cells.

PAX5-silenced MCL cells exhibit increased colony-forming capacity and bone marrow engraftment in vivo

We analyzed the colony-forming abilities of PAX5$^-$ MCL cells using phytohemagglutinin leukocyte conditioned medium (PHA-LCM), which has been used to evaluate the stem-like properties of myeloma.[25] PAX5 silencing significantly increased the number of MCL colony-forming units compared to the control treatment (Figure 2a).

We further analyzed the effect of PAX5 gene silencing on stem-like cell engraftment using PKH26 dye as described previously.[26] GFP+-expressing MCL cell engraftment was not different between PAX5$^-$ MCL and control cells after 48 hours in vivo. The PKH26+ cell recovery rate was significantly higher in PAX5$^-$ xenografts than in control xenografts (Figure 2b and Supplementary Table 2). Immunohistochemistry (IHC) analysis of bones and spleens from xenografted mice confirmed our fluorescence-activated cell sorting (FACS) findings (Figure 2c). We observed a quantitative increase of 18.2% and 35% in the engraftment of PAX5$^-$ SP53 and Jeko cells, respectively, compared to the control cells (Supplementary Table 2).

PAX5 silencing promotes tumor spread in xenografted mice

We first transplanted PAX5$^-$ MCL cells or control cells into NOD/SCID mice via intravenous injection. After 6–8 weeks, we discovered significantly greater numbers of CD45+ and GFP+ cells from the PAX5$^-$ MCL xenografted mice than in the control mice (Figure 3a and Supplementary Figure 3a). The differences in cell engraftment were particularly large in the bone marrow regardless of the number of transplanted cells (Figure 3a). IHC analyses of frozen tissue sections also displayed greater numbers of CD45+ cells in bones from PAX5$^-$ MCL xenografted mice (Supplementary Figure 3b).

We then transplanted MCL cells via subcutaneous injection. The PAX5⁻ MCL xenografted mice developed larger tumors than the control mice (Figure 3b), and this result was confirmed by FDG-PET and CT imaging analyses (Figure 3c). Detailed 18F–FDG uptake analyses showed that PAX5⁻ MCL tumors spread into various sites such as bone marrows, the thymus and lymph nodes (Figure 3d). There were also increased infiltration into gastrointestinal tissues in the PAX5⁻ MCL xenografted mice (Supplementary Figure 3c).

To further investigate the interaction between MCL cells and the microenvironment, we evaluated the effects of PAX5 silencing on cell adhesion using HS5 BMSCs. Compared to control cells, PAX5⁻ MCL cells demonstrated markedly increased cell adhesion to the HS5 cell monolayer (Figure 3e). PAX5⁻ MCL cells were more mobile than the control cells (Supplementary Figure 3d and j and Supplementary Videos 1 & 2), as the average distance travelled by PAX5⁻ MCL cells was far greater than that by the control cells (Supplementary Figure 3f).

Taken together, our data support unexpected functions of PAX5 in human B cell lymphoma; PAX5 downregulation leads to increased cell proliferation, stem-like properties, motility and cell adhesion, resulting in increased MCL cell infiltration and engraftment in the xenograft mice.

The upregulation of IL-6 leads to hyperactivated STAT3, AKT and MEK signaling in PAX5⁻ MCL cells

We next examined the pathways expressed in various hematological malignancies such as the PI3K/AKT/mTOR and MAPK/ERK signaling pathways.[27–31] Immunoblots showed strong activation of AKT/mTOR pathway signaling factors, including pmTOR, p-p70 and pAKT, and this activation could account for the increased proliferation of PAX5−MCL cells (Figure 4a). pERK and pMAPK have been implicated in cell survival, adhesion to the microenvironment and motility;[32] the levels of these factors were also increased in PAX5⁻ MCL cells (Figure 4a). Interestingly, CCND3, which encodes for cyclin D3, an important cyclin for early B cell growth,[33] was also increased (Supplementary Figure 4a).

The hyperactivation of the AKT/mTOR and MAPK/ERK signaling pathways in PAX5⁻ cells implies a possible deregulation of IL-6, an important upstream signaling protein.[34,35] The IL-6 levels were significantly increased in PAX5⁻ MCL conditioned media compared to media from control cells; HS5 conditioned medium served as a positive control (Figure 4b). Serum restriction has also been reported to induce IL-6 expression,[36] and nutrient restriction resulted in markedly increased IL-6 secretion in SP53 PAX5⁻ cells compared to control cells (Figure 4b). Alternatively, in Jeko cells, which do not produce autocrine IL-6,[36] PAX5 silencing did not increase IL-6 production (Supplementary Figure 4b). However, the levels of IL-6, GP80 (an IL-6 receptor) and GP130 (an IL-6 signal transducer) were significantly increased in both PAX5⁻ SP53 and Jeko cells compared to the corresponding control cells (Figure 4c). The mRNA levels of the downstream IL-6 targets BCL-XL, MCL1 and S1PR1 were significantly increased after serum restriction in PAX5⁻ MCL cells compared to control cells (Supplementary Figure 4c).

We used conditioned media from HS5 human BMSCs enriched for IL-6 [37] (HS5-CM) as an alternative source of paracrine IL-6. ELISA and immunoblot analyses confirmed IL-6 expression in HS5-CM (Supplementary Figure 4d). At the steady state (0 hours), PAX5$^-$ MCL cells expressed higher pSTAT3 levels, which increased upon HS5 addition compared to control cells (Figure 4d). Furthermore, treatment with IL-6 neutralizing antibodies reduced pSTAT3 activation when supplemented with HS5-CM (Figure 4e). Our data suggest that PAX5 downregulation potentiates cells to exert a greater response to exogenous IL-6, potentially leading to increased cell infiltration into the bone marrows (Figure 3a).

PAX5 silencing facilitates bortezomib resistance via plasmacytic differentiation

Doxorubicin and etoposide are commonly used chemotherapeutic agents that can induce p53-mediated cell damage responses.[38,39] The TP53 transcript levels were significantly decreased in PAX5$^-$ cells within 24 hours of doxorubicin treatment (Supplementary Figure 4e). RT-PCR analyses also showed that after 6 or 12 hours of etoposide treatment, PAX5$^-$ cells expressed lower TP53 transcript levels (Supplementary Figure 4f). As expected based on the TP53 expression responses after drug treatment, PAX5$^-$ SP53 cells were more resistant to doxorubicin treatment (Supplementary Figure 4g).

We further investigated the roles of PAX5 in MCL using the clinically therapeutic agent bortezomib. Bortezomib inhibits proteasomal activity and is widely used to treat relapsed MCL, albeit with varying clinical efficacy due to the drug resistant tumor cells.[40] PAX5$^-$ MCL cells showed increased resistance to bortezomib and bortezomib-containing regimens (Supplementary Figure 4h). PAX5$^-$ MCL cells upregulated transcription factors that determine plasmacytic differentiation, such as interferon regulatory factor 4 (IRF4) and Blimp-1, as determined by qRT-PCR (Supplementary Figure 4I) and immunoblotting (Supplementary Figure 4J). Interestingly, both qRT-PCR and immunoblotting of PAX5$^-$ Jeko cells showed no significant increase in IRF4 expression; this result was consistent with previous reports using Jeko.BR (bortezomib-resistant) subclones.[41] In addition, the expression of the plasma cell marker CD138 was increased in PAX5$^-$ MCL cells (Supplementary Figure 4K), suggesting that PAX5 downregulation promotes the resistance of MCL cells to bortezomib by facilitating plasmacytic differentiation.

PAX5 downregulation is an indicator of MCL progression and is associated with aggressive blastoid variant MCL

We conducted comprehensive PAX5 level analyses on 39 different primary MCL samples, consisting of 31 peripheral blood and 8 bone marrow aspirate specimens (Supplementary Table 3). All studies were conducted in a blinded manner, in which only CD19+ cells isolated via positive selection were analyzed. Compared to those from normal control blood or bone marrow samples, the PAX5 levels were significantly reduced in CD19+ cells from MCL patient samples (Figure 5a and b). Interestingly, the PAX5 levels in MCL CD19+ cells from bone marrow samples were significantly lower than those from blood samples (Figure 5c). To determine the experimental relevance of this result, we transplanted unmanipulated SP53 MCL cells into mice via subcutaneous injection. We observed that the PAX5 levels were significantly lower in disseminated human cells isolated from the spleen and bone marrow than in the localized parental subcutaneous tumor cells (Supplementary Figure 5a).

PAX5$^-$ MCL xenografted mice displayed tumor spread to gastrointestinal sites (Supplementary Figure 3c). Similarly, we found that the PAX5 levels in CD19+ tumor cells were significantly lower in patients with a record of gastrointestinal involvement than in patients without recorded gastrointestinal involvement (Figure 5d).

Blastoid variant MCL is a highly aggressive but rare MCL subtype that has a worse prognosis than the more common forms of MCL.[42–44] Analysis of patient samples revealed that blastoid MCL cases contained significantly reduced PAX5 levels compared to non-blastoid MCL cases (Figure 5e). We then analyzed the CCND1 levels in these samples and found at least a 4-fold increase in expression compared to normal B cells (Supplementary Table 4 and Supplementary Figure 5b). However, further correlation analysis revealed that CCND1 expression could not predict the survival of MCL patients between blastoid variant and non-blastoid variant MCL (Supplementary Figure 5c). Moreover, we found that the overall survival of patients displaying PAX5^{low} was significantly lower than that of patients displaying PAX5^{high} (Figure 5f, Supplementary Table 5). The PAX5^{low} patients exhibited a survival rate very similar to that of the verified blastoid MCL cases within our data set (Supplementary Figure 5d), suggesting that the PAX5 levels can be used to predict survival among advanced MCL patients. Collectively, our data support PAX5 downregulation as an important signaling event in MCL that contributes to the enhanced progression and infiltration of malignant B cells.

High throughput screening (HTS) of compounds reveals the drug-resistant nature of PAX5$^-$ MCL cells

To further support our understanding regarding the drug-resistant nature of PAX5-silenced MCL cells, we screened 3864 compounds from three different libraries: a custom made library (Custom Clinical, 246 compounds), a bioactive library containing FDA-approved compounds (Prestwick, 1200 compounds) and an NCI diversity library containing compounds currently under development or in clinical trials (NCI Diversity library, 2418 compounds) (Supplementary Figure 6a). A consistent Z' score of >0.5 across different screening days indicated that the screen was consistent and reliable.[45] A high signal-to-noise ratio was achieved for all three libraries, and a scatterplot for each cell type depicted a clear distinction between the control and test compounds (Supplementary Figure 6b–d).

Compounds that displayed a difference in efficacy of at least 5% between control and PAX5$^-$ MCL cells were analyzed. After filtering the compounds displaying at least 40% of the inhibitory effect of doxorubicin (HTS positive control), we obtained a positive hit rate of 3.7% – 7.0% of the compounds in the HTS libraries. Across all three libraries, the PAX5$^-$ MCL cells were much more resistant than the control cells (Figure 6a). Further analysis revealed many unique compounds to which PAX5$^-$ MCL cells were resistant (Figure 6b–d); these compounds were selected based on their significance as detailed in the Supplementary Methods. We further analyzed the compounds to which PAX5$^-$ MCL cells were resistant and linked these compounds to known biological pathways. Compounds that targeted the PI3K–AKT-mTOR and MEK/ERK signaling cascades were less effective in killing PAX5$^-$ Jeko cells compared to control cells (Figure 6e). A similar trend was observed for PAX5$^-$ SP53 cells (Supplementary Figure 6e), suggesting that PAX5$^-$ MCL cells utilize

hyperactivated PI3K–AKT-mTOR and MEK/ERK signaling pathways to promote their survival.

Discussion

Despite its essential roles in determining and maintaining B cell identity in mice,[4] the functions of PAX5 in human B malignancies are unclear. We found quantitative differences in PAX5 expression between normal B cells and B cells from MCL patients, which displayed decreased PAX5 levels (Figure 5a–b). In MCL patients, PAX5 levels were decreased in lymphoma cells from bone marrow compared to those from peripheral blood (Figure 5c). In xenografted mice, subcutaneous tumor cells contained higher PAX5 levels than human B cells from bone marrow (Supplementary Figure 5a). These data support PAX5 downregulation in B cells as an important event for their conversion to malignant B cells and their dispersal during disease progression. However, PAX5 was not absent from MCL cells, suggesting that reduced PAX5 levels may be sufficient to induce global changes in gene expression that result in tumor transformation and progression. When we analyzed the PAX5 levels in the existing MCL database,[46] we were unable to detect a correlation between the PAX5 levels and patient survival. This discrepancy could be due to differences in the methods used to generate the data: the existing database used lymph node biopsies from patients, and these samples contain non-B cells and supporting stromal cells. In contrast, our data were based on purified CD19+ B cells. It remains possible that the B cells that we collected contained normal B cells. However, all MCL samples that we used were stage 4 with extranodal site involvement; thus, the number of normal B cells in each sample was minimal.

The downregulation of PAX5 levels in tumor cells upon infiltration and dissemination suggests that the levels are controlled by epigenetic mechanisms rather than genetic translocation or deletion, as shown in ALL.[11] When we analyzed MCL cells for known PAX5 translocations, none were detected (data not shown). The quantitative differences in the PAX5 expression levels between the tissues collected from MCL patients prompted us to silence the PAX5 gene in MCL cell lines, which are of peripheral blood origin, to characterize the functions of PAX5 in MCL progression.

PAX5$^-$ MCL cells showed markedly increased proliferation in vitro and in vivo, whereas PAX5-overexpressing cells exhibited delayed growth and cell death (Figure 1a–b). Increased cell proliferation was accompanied by changes in the cell cycle and several cell cycle-related genes, such as increased expression of CDKs and decreased expression of tumor suppressor genes such as Rb (Figure 1g). It is likely that the collective upregulation of cell cycle-promoting genes and downregulation of cell cycle-suppressing genes such as Rb, p53, p21 and p27 contribute to the increased proliferation of PAX5$^-$ MCL cells.

PAX5$^-$ MCL cells also utilized the hyperactivity of existing prosurvival pathways, including the AKT/mTOR and MAPK/ERK pathways, to promote their growth (Figure 4a). It is likely that IL-6 acts upstream of these pathways because PAX5$^-$ SP53 cells produced more IL-6 than control cells (Figure 4b). The possible roles of platelet-derived growth factor receptor (PDGFR) and epithelial growth factor receptor (EGFR) on PAX5$^-$ MCL signaling should be

further explored. PDGFR has been implicated in increased AKT and STAT3 signaling,[47] and both PDGFR and EGFR have been reported to synergize with IL-6 signaling, possibly leading to increased IL-6 signal sensitivity.[48–50] IL-6-related downstream genes were even upregulated in Jeko cells, which do not produce IL-6, suggesting that PAX5 can influence IL-6-related gene expression. In multiple myeloma (MM) KAS 6/1 cells, IL-6 treatment leads to TP53 promoter methylation, resulting in decreased TP53 expression levels.[51] Therefore, increased autocrine IL-6 expression in PAX5$^-$ MCL cells may contribute to the reduction in TP53 gene expression via promoter hypermethylation.

Stromal cells likely represent the primary source of paracrine IL-6 in bone marrow, as co-culturing PAX5$^-$ MCL cells with HS-5 cells led to the upregulation of pSTAT3 signaling (Figure 4d). Advanced MCL patients often show the involvement of extranodal sites, such as bone marrow, and for malignant cells to survive in tissues other than their tissue of origin, adaptation to the local microenvironment is necessary. Increased autocrine IL-6 levels upon PAX5 silencing could provide survival advantages to MCL cells in an environment that lacks a source of paracrine IL-6. Therefore, PAX5 downregulation could serve as an adaptive process that promotes survival in the local microenvironment.

PAX5−/− pro-B cells display increased lineage plasticity and differentiation into functional macrophages, granulocytes, dendritic cells, osteoclasts and natural killer cells in vivo.[7, 8] Adoptive transfer of PAX5−/− B cells to immunodeficient mice led to the development of T cells, indicating that Pax5 downregulation induces mature B cells to acquire a plasticity that is similar to that of early progenitor cells. We did not directly examine the lineage differentiation of PAX5$^-$ MCL cells due to other oncogenic mutations; however, the MCL cells exhibited significantly increased colony-forming ability in PHA-LCM medium upon PAX5 silencing. In addition, transferring PKH26+ PAX5$^-$ MCL cells to xenografted mice increased the number of quiescent PKH26+ cells in these mice, indicating that PAX5 silencing in MCL affects the retention of quiescent cells. PKH26 labelling has been utilized to isolate long-term HSCs and cancer stem cells in some cancer types.[52] Our data support the concept that PAX5 downregulation promotes MCL cells to exhibit a more stem-like phenotype. However, the detailed molecular mechanisms underlying this process remain to be evaluated by RNA-seq or CHIP-seq.

Our HTS results further clarify the drug-resistant nature of PAX5$^-$ MCL cells. In particular, PAX5$^-$ MCL cells were highly resistant to compounds that target PI3K/AKT/mTOR-, MEK/ERK-, PDGFR- and EGFR-related pathways (Figure 6e). Interestingly, fewer drugs killed TP53-null Jeko cells compared to wild type SP53 cells, suggesting that the TP53 mutational status could impact drug resistance in MCL. The compounds that we identified may serve as good candidates for novel MCL patient therapies; we plan to perform additional pre-clinical studies to narrow down this list of compounds for further studies.

Our discovery of a correlation of PAX5 levels with aggressive blastoid MCL is the first evidence of the clinical importance of reduced PAX5 levels to lymphoma progression. Our data also suggest that the PAX5 levels could be used as a prognostic marker for MCL patients. Collectively, our findings provide novel insight into the functions of PAX5 in

human B cell cancer and support a paradigm shift in understanding the pathogenesis of MCL.

Supplementary Material

Refer to Web version on PubMed Central for supplementary material.

REFERENCE

1. Hagman J, Lukin K. Transcription factors drive B cell development. Current opinion in immunology. 2006 Apr; 18(2):127–134. [PubMed: 16464566]
2. Czerny T, Schaffner G, Busslinger M. DNA sequence recognition by Pax proteins: bipartite structure of the paired domain and its binding site. Genes & development. 1993 Oct; 7(10):2048–2061. [PubMed: 8406007]
3. Dorfler P, Busslinger M. C-terminal activating and inhibitory domains determine the transactivation potential of BSAP (Pax-5), Pax-2 and Pax-8. The EMBO journal. 1996 Apr 15;15(8):1971–1982. [PubMed: 8617244]
4. Cobaleda C, Schebesta A, Delogu A, Busslinger M. Pax5: the guardian of B cell identity and function. Nat Immunol. 2007 May; 8(5):463–470. [PubMed: 17440452]
5. Nutt SL, Heavey B, Rolink AG, Busslinger M. Commitment to the B-lymphoid lineage depends on the transcription factor Pax5. Nature. 1999 Oct 7;401(6753):556–562. [PubMed: 10524622]
6. Delogu A, Schebesta A, Sun Q, Aschenbrenner K, Perlot T, Busslinger M. Gene repression by Pax5 in B cells is essential for blood cell homeostasis and is reversed in plasma cells. Immunity. 2006 Mar; 24(3):269–281. [PubMed: 16546096]
7. Mikkola I, Heavey B, Horcher M, Busslinger M. Reversion of B cell commitment upon loss of Pax5 expression. Science. 2002 Jul 5; 297(5578):110–113. [PubMed: 12098702]
8. Schaniel C, Bruno L, Melchers F, Rolink AG. Multiple hematopoietic cell lineages develop in vivo from transplanted Pax5-deficient pre-B I-cell clones. Blood. 2002 Jan 15; 99(2):472–478. [PubMed: 11781227]
9. Hoflinger S, Kesavan K, Fuxa M, Hutter C, Heavey B, Radtke F, et al. Analysis of Notch1 function by in vitro T cell differentiation of Pax5 mutant lymphoid progenitors. Journal of immunology. 2004 Sep 15; 173(6):3935–3944.
10. Morrison AM, Jager U, Chott A, Schebesta M, Haas OA, Busslinger M. Deregulated PAX-5 transcription from a translocated IgH promoter in marginal zone lymphoma. Blood. 1998 Nov 15; 92(10):3865–3878. [PubMed: 9808580]
11. Mullighan CG, Goorha S, Radtke I, Miller CB, Coustan-Smith E, Dalton JD, et al. Genome-wide analysis of genetic alterations in acute lymphoblastic leukaemia. Nature. 2007 Apr 12; 446(7137): 758–764. [PubMed: 17344859]
12. Cobaleda C, Jochum W, Busslinger M. Conversion of mature B cells into T cells by dedifferentiation to uncommitted progenitors. Nature. 2007 Sep 27; 449(7161):473–477. [PubMed: 17851532]
13. Vose JM. Mantle cell lymphoma: 2012 update on diagnosis, risk-stratification, and clinical management. American journal of hematology. 2012 Jun; 87(6):604–609. [PubMed: 22615102]
14. Salaverria I, Perez-Galan P, Colomer D, Campo E. Mantle cell lymphoma: from pathology and molecular pathogenesis to new therapeutic perspectives. Haematologica. 2006 Jan; 91(1):11–16. [PubMed: 16434365]
15. Adams JM, Harris AW, Strasser A, Ogilvy S, Cory S. Transgenic models of lymphoid neoplasia and development of a pan-hematopoietic vector. Oncogene. 1999 Sep 20; 18(38):5268–5277. [PubMed: 10498879]
16. Bodrug SE, Warner BJ, Bath ML, Lindeman GJ, Harris AW, Adams JM. Cyclin D1 transgene impedes lymphocyte maturation and collaborates in lymphomagenesis with the myc gene. The EMBO journal. 1994 May 1; 13(9):2124–2130. [PubMed: 8187765]

17. Kastan MB, Bartek J. Cell-cycle checkpoints and cancer. Nature. 2004 Nov 18; 432(7015):316–323. [PubMed: 15549093]
18. Malumbres M, Barbacid M. Mammalian cyclin-dependent kinases. Trends in biochemical sciences. 2005 Nov; 30(11):630–641. [PubMed: 16236519]
19. Massague J. G1 cell-cycle control and cancer. Nature. 2004 Nov 18; 432(7015):298–306. [PubMed: 15549091]
20. Chilosi M, Doglioni C, Magalini A, Inghirami G, Krampera M, Nadali G, et al. p21/WAF1 cyclin-kinase inhibitor expression in non-Hodgkin's lymphomas: a potential marker of p53 tumor-suppressor gene function. Blood. 1996 Nov 15; 88(10):4012–4020. [PubMed: 8916968]
21. Sanchez-Beato M, Sanchez-Aguilera A, Piris MA. Cell cycle deregulation in B-cell lymphomas. Blood. 2003 Feb 15; 101(4):1220–1235. [PubMed: 12393483]
22. Ding BC, Whetstine JR, Witt TL, Schuetz JD, Matherly LH. Repression of human reduced folate carrier gene expression by wild type p53. The Journal of biological chemistry. 2001 Mar 23; 276(12):8713–8719. [PubMed: 11106643]
23. Drakos E, Atsaves V, Li J, Leventaki V, Andreeff M, Medeiros LJ, et al. Stabilization and activation of p53 downregulates mTOR signaling through AMPK in mantle cell lymphoma. Leukemia : official journal of the Leukemia Society of America, Leukemia Research Fund, UK. 2009 Apr; 23(4):784–790.
24. Pridans C, Holmes ML, Polli M, Wettenhall JM, Dakic A, Corcoran LM, et al. Identification of Pax5 target genes in early B cell differentiation. Journal of immunology. 2008 Feb 1; 180(3):1719–1728.
25. Matsui W, Huff CA, Wang Q, Malehorn MT, Barber J, Tanhehco Y, et al. Characterization of clonogenic multiple myeloma cells. Blood. 2004 Mar 15; 103(6):2332–2336. [PubMed: 14630803]
26. Chen Z, Orlowski RZ, Wang M, Kwak L, McCarty N. Osteoblastic niche supports the growth of quiescent multiple myeloma cells. Blood. 2014 Jan 14.
27. Carlo-Stella C, Locatelli SL, Giacomini A, Cleris L, Saba E, Righi M, et al. Sorafenib inhibits lymphoma xenografts by targeting MAPK/ERK and AKT pathways in tumor and vascular cells. PloS one. 2013; 8(4):e61603. [PubMed: 23620775]
28. Dal Col J, Zancai P, Terrin L, Guidoboni M, Ponzoni M, Pavan A, et al. Distinct functional significance of Akt and mTOR constitutive activation in mantle cell lymphoma. Blood. 2008 May 15; 111(10):5142–5151. [PubMed: 18339899]
29. Dennison JB, Shanmugam M, Ayres ML, Qian J, Krett NL, Medeiros LJ, et al. 8-Aminoadenosine inhibits Akt/mTOR and Erk signaling in mantle cell lymphoma. Blood. 2010 Dec 16; 116(25): 5622–5630. [PubMed: 20844237]
30. Psyrri A, Papageorgiou S, Liakata E, Scorilas A, Rontogianni D, Kontos CK, et al. Phosphatidylinositol 3'-kinase catalytic subunit alpha gene amplification contributes to the pathogenesis of mantle cell lymphoma. Clinical cancer research : an official journal of the American Association for Cancer Research. 2009 Sep 15; 15(18):5724–5732. [PubMed: 19723646]
31. Wang M, Atayar C, Rosati S, Bosga-Bouwer A, Kluin P, Visser L. JNK is constitutively active in mantle cell lymphoma: cell cycle deregulation and polyploidy by JNK inhibitor SP600125. The Journal of pathology. 2009 May; 218(1):95–103. [PubMed: 19206150]
32. Kolch W. Coordinating ERK/MAPK signalling through scaffolds and inhibitors. Nature reviews Molecular cell biology. 2005 Nov; 6(11):827–837. [PubMed: 16227978]
33. Cooper AB, Sawai CM, Sicinska E, Powers SE, Sicinski P, Clark MR, et al. A unique function for cyclin D3 in early B cell development. Nat Immunol. 2006 May; 7(5):489–497. [PubMed: 16582912]
34. Nagel S, Scherr M, Quentmeier H, Kaufmann M, Zaborski M, Drexler HG, et al. HLXB9 activates IL6 in Hodgkin lymphoma cell lines and is regulated by PI3K signalling involving E2F3. Leukemia : official journal of the Leukemia Society of America, Leukemia Research Fund, UK. 2005 May; 19(5):841–846.

35. Patil C, Zhu X, Rossa C Jr, Kim YJ, Kirkwood KL. p38 MAPK regulates IL-1beta induced IL-6 expression through mRNA stability in osteoblasts. Immunological investigations. 2004 May; 33(2):213–233. [PubMed: 15195698]
36. Zhang L, Yang J, Qian J, Li H, Romaguera JE, Kwak LW, et al. Role of the microenvironment in mantle cell lymphoma: IL-6 is an important survival factor for the tumor cells. Blood. 2012 Nov 1; 120(18):3783–3792. [PubMed: 22968454]
37. Graf L, Iwata M, Torok-Storb B. Gene expression profiling of the functionally distinct human bone marrow stromal cell lines HS-5 and HS-27a. Blood. 2002 Aug 15; 100(4):1509–1511. [PubMed: 12184274]
38. Karpinich NO, Tafani M, Rothman RJ, Russo MA, Farber JL. The course of etoposide-induced apoptosis from damage to DNA and p53 activation to mitochondrial release of cytochrome c. The Journal of biological chemistry. 2002 May 10; 277(19):16547–16552. [PubMed: 11864976]
39. Manna SK, Gangadharan C, Edupalli D, Raviprakash N, Navneetha T, Mahali S, et al. Ras puts the brake on doxorubicin-mediated cell death in p53-expressing cells. The Journal of biological chemistry. 2011 Mar 4; 286(9):7339–7347. [PubMed: 21156795]
40. Suh KS, Goy A. Bortezomib in mantle cell lymphoma. Future oncology. 2008 Apr; 4(2):149–168. [PubMed: 18407730]
41. Perez-Galan P, Mora-Jensen H, Weniger MA, Shaffer AL 3rd, Rizzatti EG, Chapman CM, et al. Bortezomib resistance in mantle cell lymphoma is associated with plasmacytic differentiation. Blood. 2011 Jan 13; 117(2):542–552. [PubMed: 20956803]
42. Argatoff LH, Connors JM, Klasa RJ, Horsman DE, Gascoyne RD. Mantle cell lymphoma: a clinicopathologic study of 80 cases. Blood. 1997 Mar 15; 89(6):2067–2078. [PubMed: 9058729]
43. Bernard M, Gressin R, Lefrere F, Drenou B, Branger B, Caulet-Maugendre S, et al. Blastic variant of mantle cell lymphoma: a rare but highly aggressive subtype. Leukemia : official journal of the Leukemia Society of America, Leukemia Research Fund, UK. 2001 Nov; 15(11):1785–1791.
44. Bosch F, Lopez-Guillermo A, Campo E, Ribera JM, Conde E, Piris MA, et al. Mantle cell lymphoma: presenting features, response to therapy, and prognostic factors. Cancer. 1998 Feb 1; 82(3):567–575. [PubMed: 9452276]
45. Iversen, PW.; Beck, B.; Chen, YF.; Dere, W.; Devanarayan, V.; Eastwood, BJ., et al. HTS Assay Validation. Sittampalam, GS.; Gal-Edd, N.; Arkin, M.; Auld, D.; Austin, C.; Bejcek, B., editors. Bethesda (MD): Assay Guidance Manual; 2004.
46. Rosenwald A, Wright G, Wiestner A, Chan WC, Connors JM, Campo E, et al. The proliferation gene expression signature is a quantitative integrator of oncogenic events that predicts survival in mantle cell lymphoma. Cancer cell. 2003 Feb; 3(2):185–197. [PubMed: 12620412]
47. Laimer D, Dolznig H, Kollmann K, Vesely PW, Schlederer M, Merkel O, et al. PDGFR blockade is a rational and effective therapy for NPM-ALK-driven lymphomas. Nature medicine. 2012 Nov; 18(11):1699–1704.
48. Colomiere M, Ward AC, Riley C, Trenerry MK, Cameron-Smith D, Findlay J, et al. Cross talk of signals between EGFR and IL-6R through JAK2/STAT3 mediate epithelial-mesenchymal transition in ovarian carcinomas. British journal of cancer. 2009 Jan 13; 100(1):134–144. [PubMed: 19088723]
49. Wang Y, van Boxel-Dezaire AH, Cheon H, Yang J, Stark GR. STAT3 activation in response to IL-6 is prolonged by the binding of IL-6 receptor to EGF receptor. Proceedings of the National Academy of Sciences of the United States of America. 2013 Oct 15; 110(42):16975–16980. [PubMed: 24082147]
50. Wu E, Palmer N, Tian Z, Moseman AP, Galdzicki M, Wang X, et al. Comprehensive dissection of PDGF-PDGFR signaling pathways in PDGFR genetically defined cells. PloS one. 2008; 3(11):e3794. [PubMed: 19030102]
51. Hodge DR, Peng B, Cherry JC, Hurt EM, Fox SD, Kelley JA, et al. Interleukin 6 supports the maintenance of p53 tumor suppressor gene promoter methylation. Cancer research. 2005 Jun 1; 65(11):4673–4682. [PubMed: 15930285]
52. Pece S, Tosoni D, Confalonieri S, Mazzarol G, Vecchi M, Ronzoni S, et al. Biological and molecular heterogeneity of breast cancers correlates with their cancer stem cell content. Cell. 2010 Jan 8; 140(1):62–73. [PubMed: 20074520]

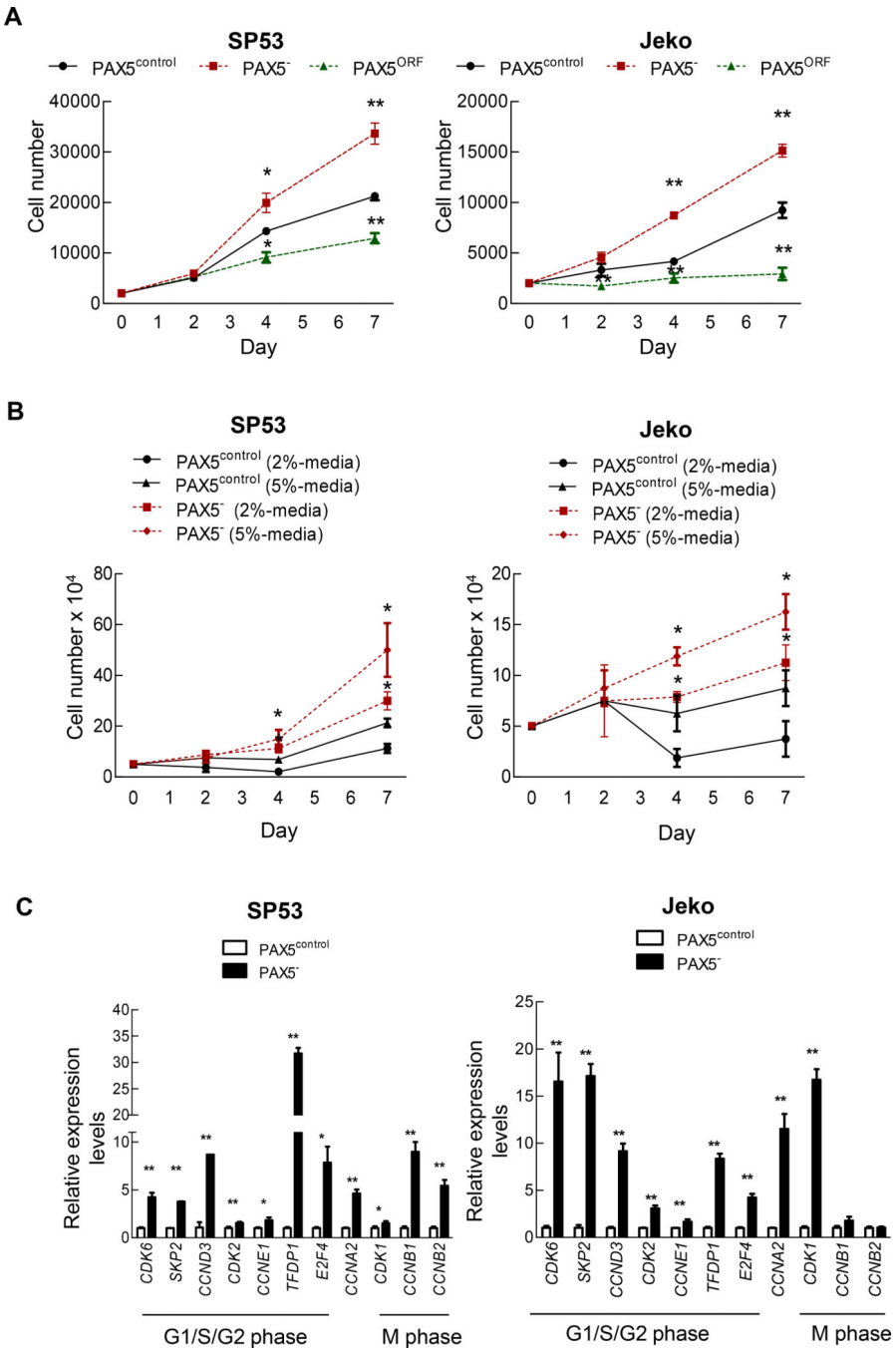

Figure 1a

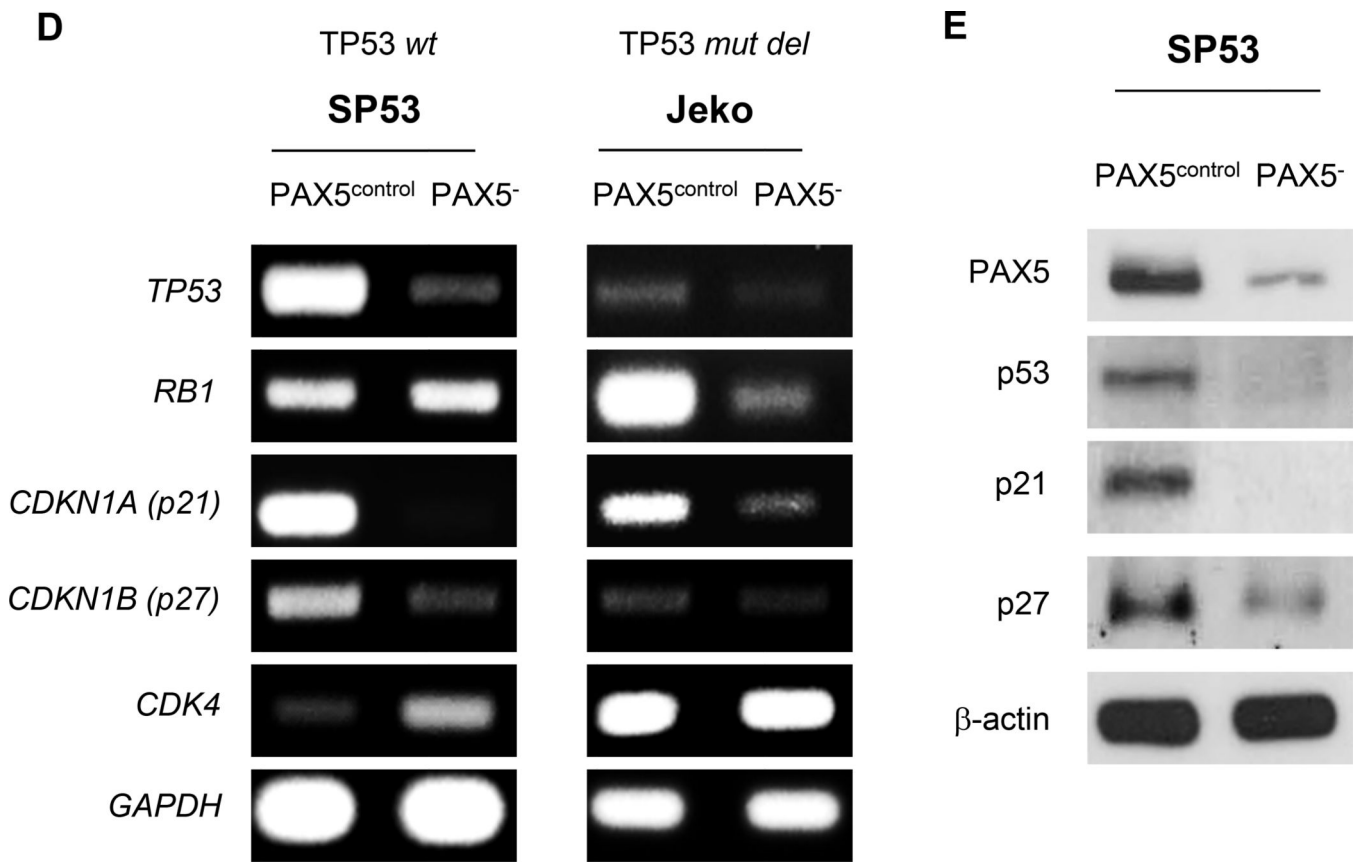

Figure 1b

Figure 1. PAX5 silencing in MCL cells leads to increased cell proliferation, and PAX5 overexpression leads to cell death

(A) PAX5^{-} cells were initially seeded at 2×10^{3} cells and were cultured for 7 days. Viable cells were counted using Trypan Blue staining at days 0, 2, 4 and 7. Each value represents the mean ± S.D. (n=3). **(B)** PAX5^{-} cells (5×10^{4}) were cultured under two different low-serum conditions and were cultured for 7 days. Viable cells were counted using Trypan Blue staining at days 0, 2, 4 and 7. Each value represents the mean ± S.D. (n=3). (**C**) qPCR analysis of cell cycle-related genes in PAX5^{-} cells. The values were normalized to β-actin. Each qRT value represents the mean ± S.D. (n=3). **(D)** Semiquantitative RT-PCR analysis showing the dysregulation of potential cell cycle inhibitors upon PAX5 silencing. SP53 cells harbor wild type TP53, and Jeko cells harbor a TP53 deletion mutant. GAPDH served as a loading control. **(E)** Immunoblot analyses of the cell cycle inhibitors p53, p27 and p21 in PAX5^{-} and control cells; β-actin served as the loading control. All cells used in these experiments were selected based on positive GFP expression, and stable cell lines were generated via antibiotic selection. *$p < 0.05$ (vs. PAX5^{control}; Student's *t*-test); **$p < 0.005$ (vs. PAX5^{control}; Student's *t*-test).

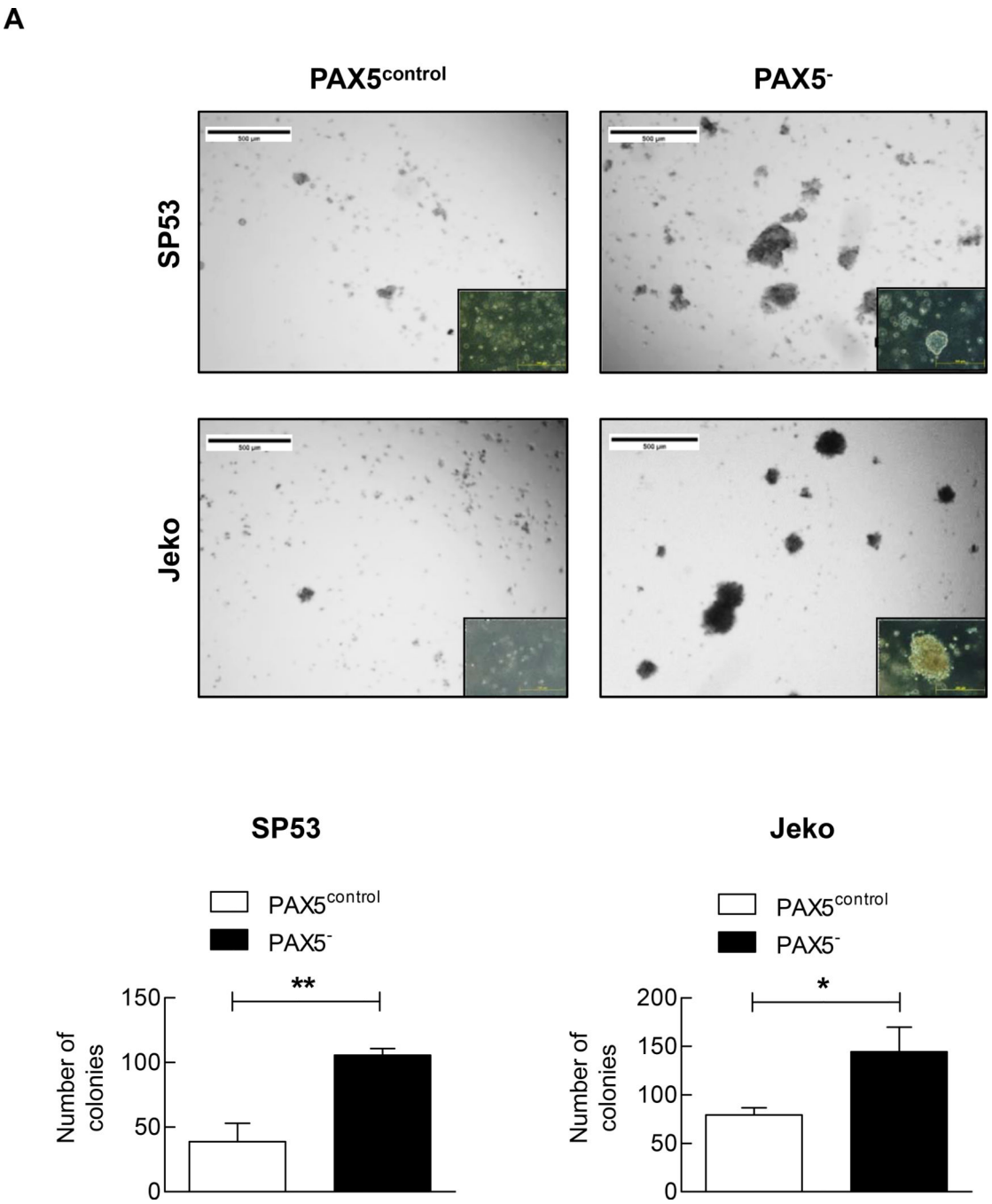

Figure 2a

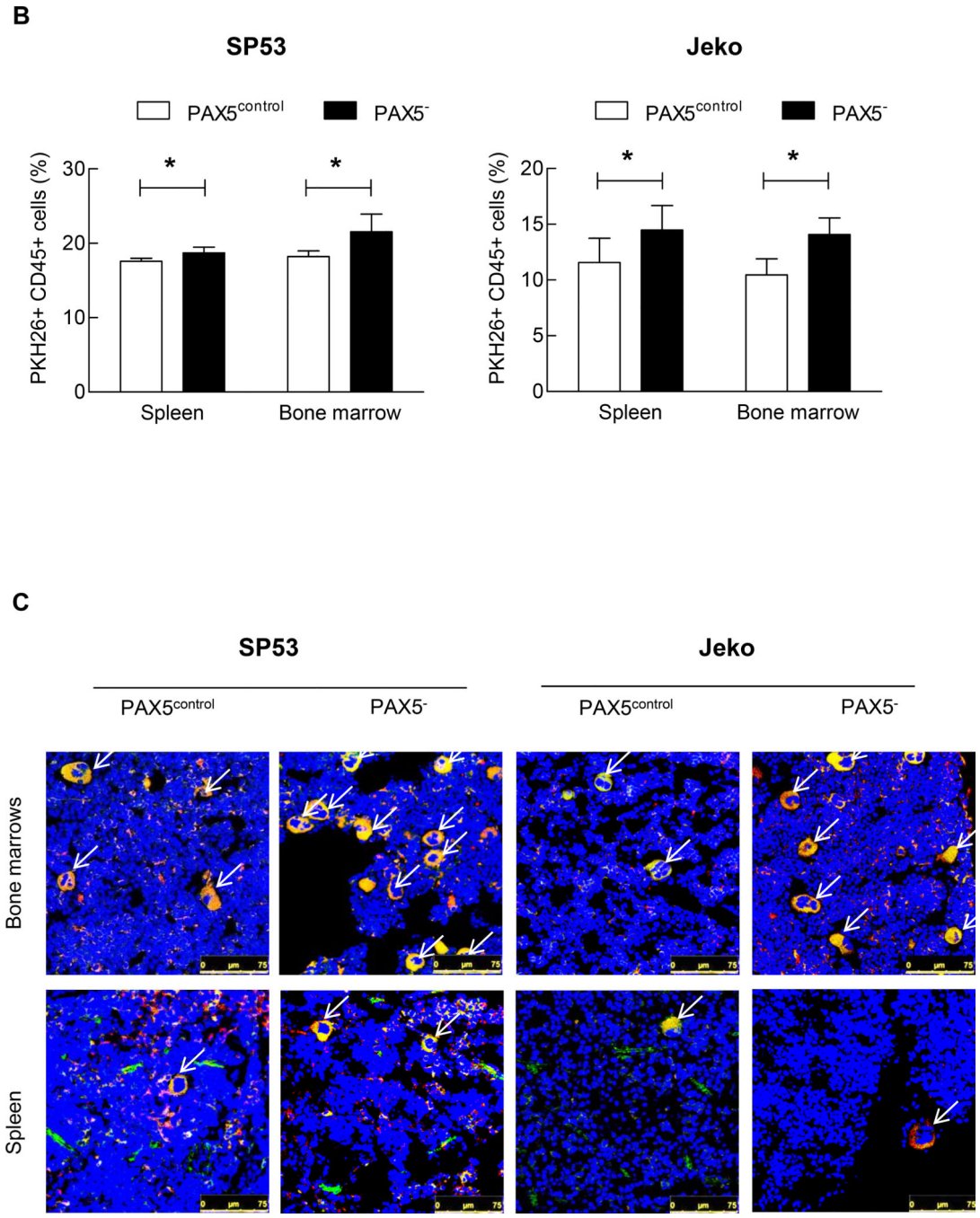

Figure 2b

Figure 2. PAX5^{-} cells demonstrate increased colony formation and PKH26+ cell retention in xenografted mice

(A) PAX5^{-} cells (5×10^{3}) were seeded in PHA-LCM, and colonies were scored at day 7. Only colonies containing > 50 cells were assigned a positive score. Inset: PAX5^{-} cells also formed larger colonies in PHA-LCM, as visualized using a light microscope with a 20x objective. Each value represents the mean number of counted colonies ± S.D. (n=3). Lower panel: The counted colonies of SP53 cells (*Left*) and Jeko cells (*Right*) were represented in a

graph. PAX5^{-} cells exhibited higher mean numbers of colonies formed ± S.D. (n=3). **(B)** PAX5^{-} cells displayed increased PKH26+ cell retention in xenografted mice. PKH26+ GFP + PAX5^{-} cells (1×10^{6}) were I.V. transferred to NOD/SCID mice. The mice were sacrificed 48 hours after injection, and cells were collected from bone marrow (femurs and tibias) and the spleen. The FACS analysis results are representative of 4 biological replicates. **(C)** Representative confocal images of GFP- and PKH-positive cells are shown. The images are merged from three different channels (DAPI, RFP and GFP) to better visualize and contrast human cells in a murine microenvironment. The arrows indicate GFP- and human PKH (RFP)-positive cells, and all cells were stained with the nucleic acid stain DAPI. Scale bar, 75 μm.

*$p < 0.05$ (vs. PAX5^{control}; Student's *t*-test); **$p < 0.005$ (vs. PAX5^{control}; Student's *t*-test).

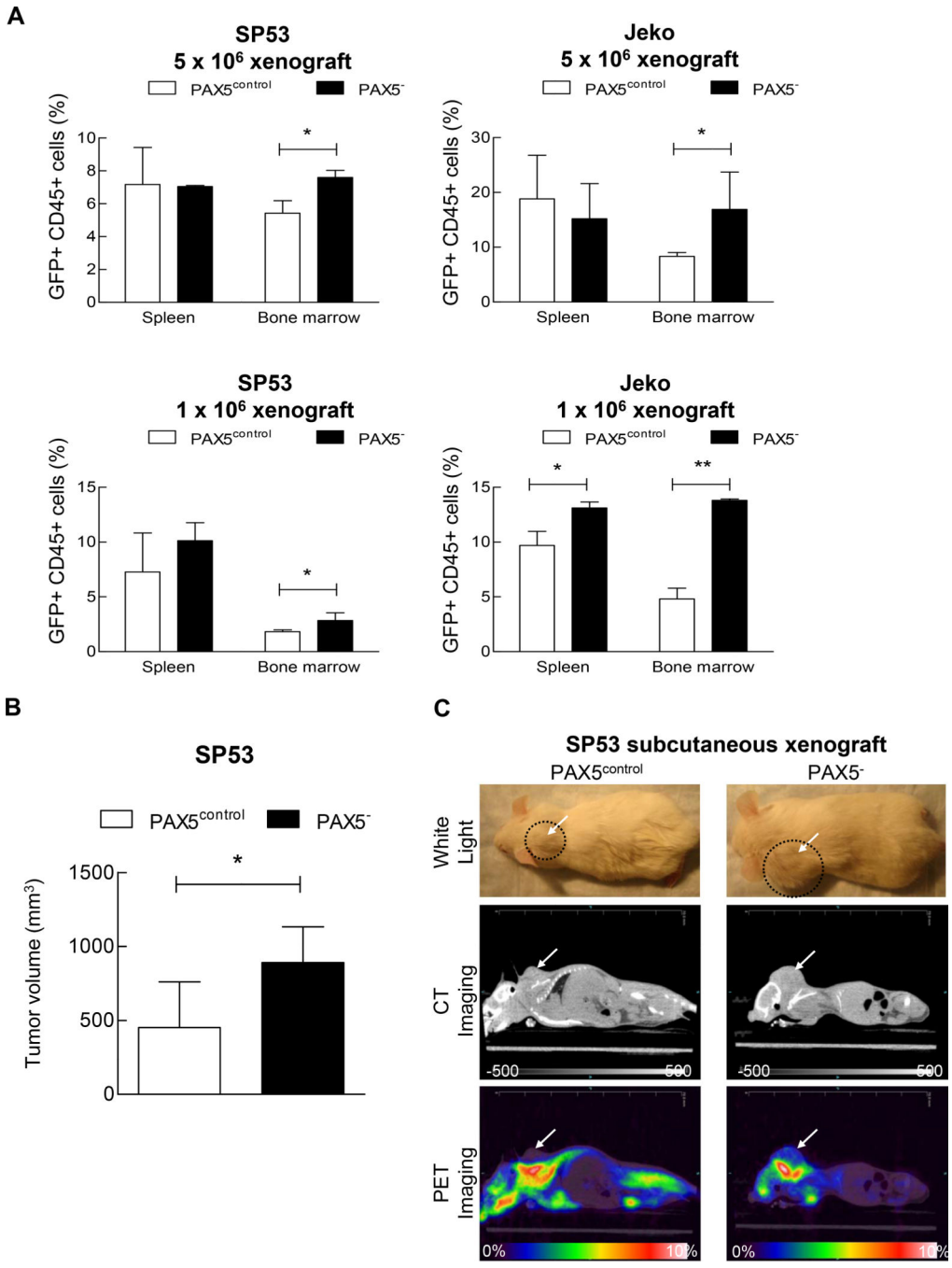

Figure 3a

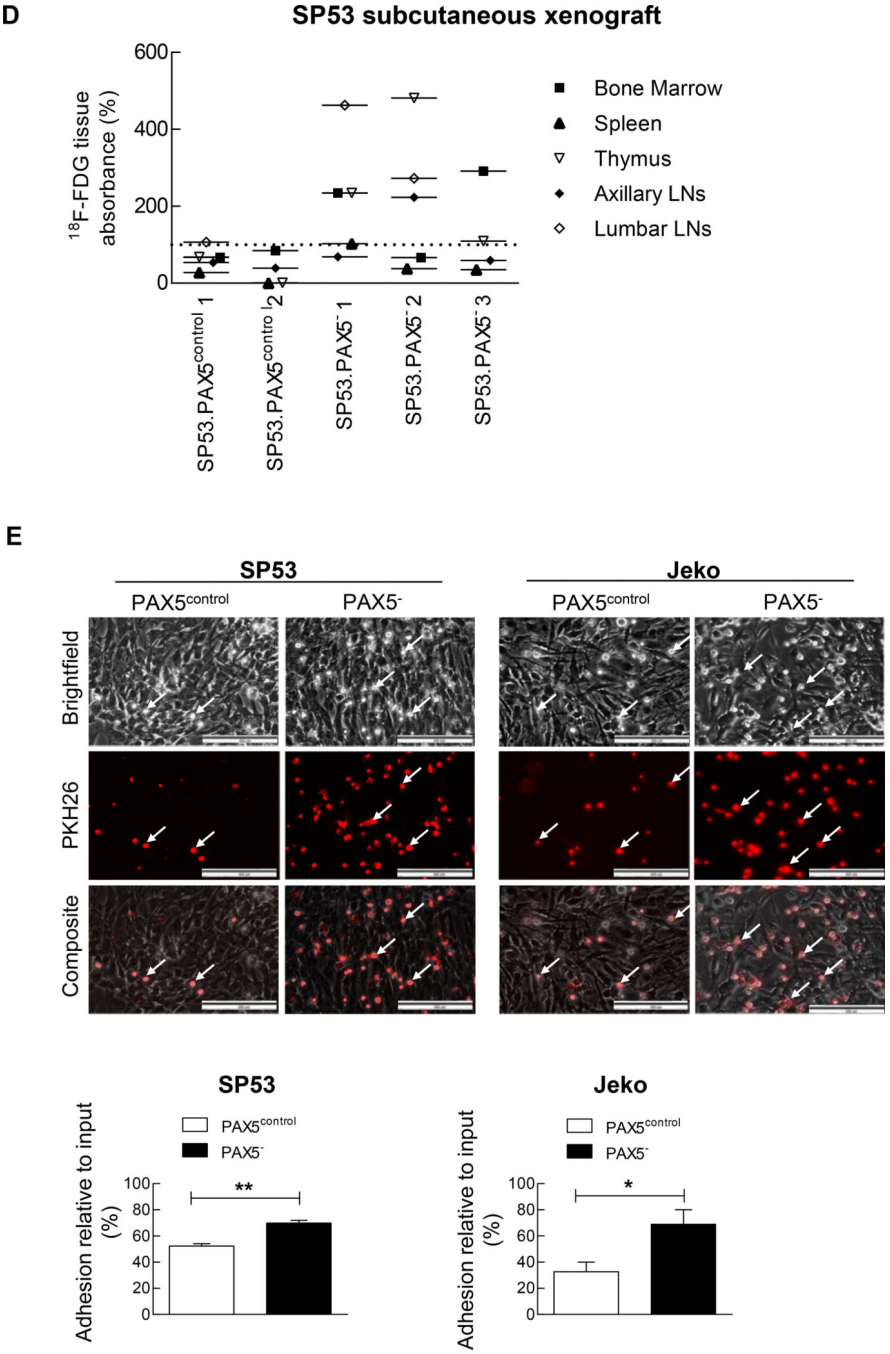

Figure 3b

Figure 3. Increased tumor cell engraftment in PAX5⁻ MCL xenografted mice

(A) PAX5⁻ MCL cells or control cells were I.V. injected into NOD/SCID mice (n=22) at two different dosages (1×10^6 or 5×10^6 cells). After 8 weeks, the xenografted mice were sacrificed. Bone marrow (femurs and tibias) and the spleen were collected and stained for human leukocyte cells using an anti-CD45 antibody. The samples were then analyzed for GFP+ and CD45+ cells using FACS. **(B)** PAX5⁻ MCL cells (3×10^6) or control cells were subcutaneously injected into NOD/SCID mice (n=9), and the tumor volumes were measured

using a digital caliper after 4 weeks. **(C)** CT and PET imaging revealed that PAX5^{-} MCL cells formed larger subcutaneous tumors in vivo. ^{18}F-FDG was injected into mice 2.5 hours prior to PET and CT imaging. Representative animals for each experimental arm are displayed in white light (*Top*), on CT (*Middle*) and on PET (*Bottom*). The white arrows indicate a subcutaneous tumor; the dotted circles represent the area of the subcutaneous tumor. CT imaging scale bar: Hounsfield scale; PET imaging scale bar: %ID/g. **(D)** ^{18}F-FDG counts of common MCL dissemination organ sites from SP53 PAX5^{-} or control subcutaneous xenografts. The %ID/g of each target organ was normalized to that of muscle tissue. The dotted line represents the percentage of ^{18}F-FDG uptake relative to muscle (muscle = 100%). Sub-cu = subcutaneous; LN = lymph node. **(E)** PAX5^{-} MCL cells were stained for PKH26 and subsequently seeded on a pre-established monolayer of HS5 bone marrow stromal cells. The arrows indicate PKH26^{+} cells. Scale bar, 200 μm. Lower panel: The adhesion of lymphoma cells was calculated by measuring the PKH26 dye intensity relative to the fluorescence of the inputs. Each value represents the mean ± S.D. (n=6). *$p < 0.05$ (vs. PAX5^{control}; Student's *t*-test); **$p < 0.005$ (vs. PAX5^{control}; Student's *t*-test).

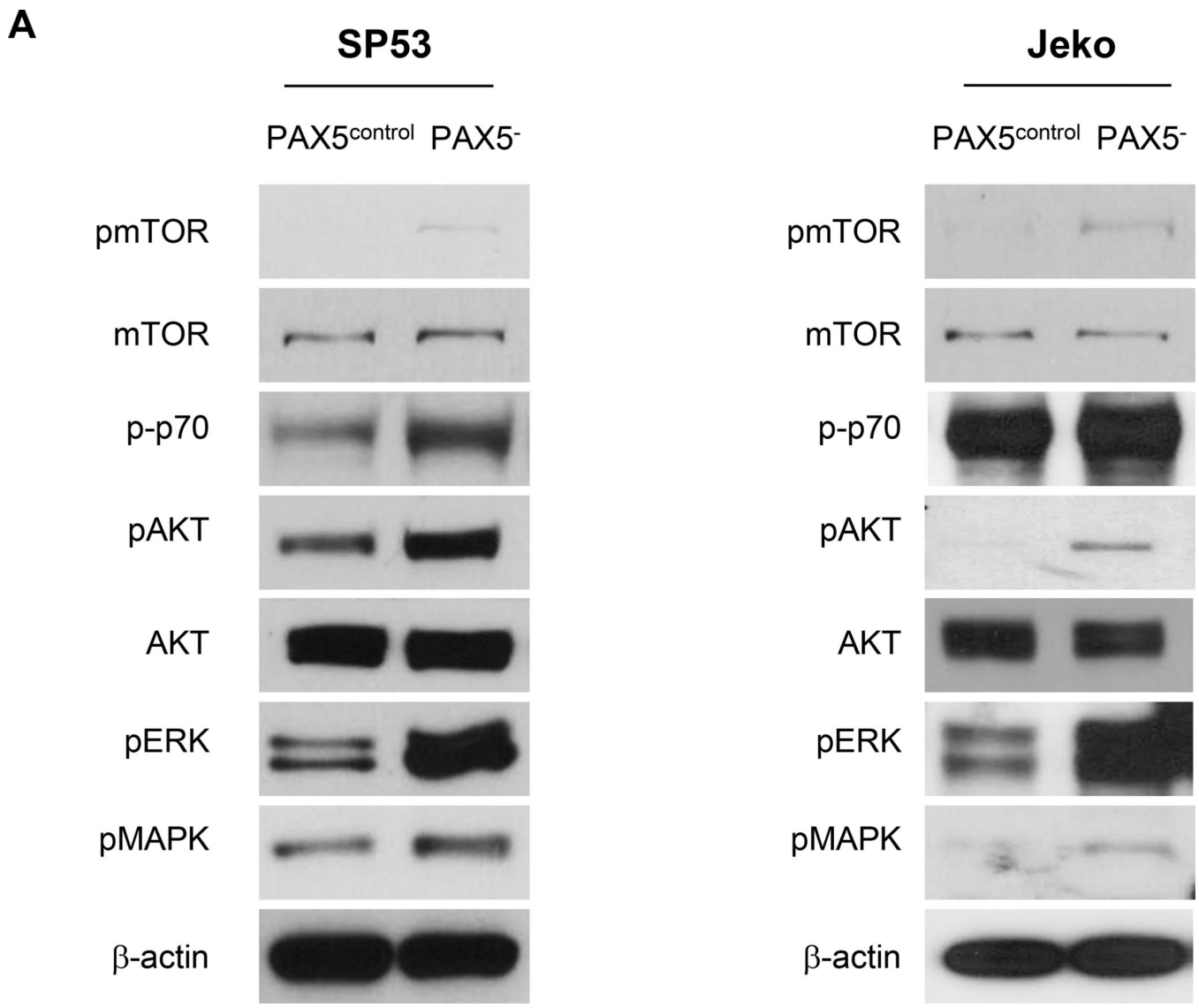

Figure 4a

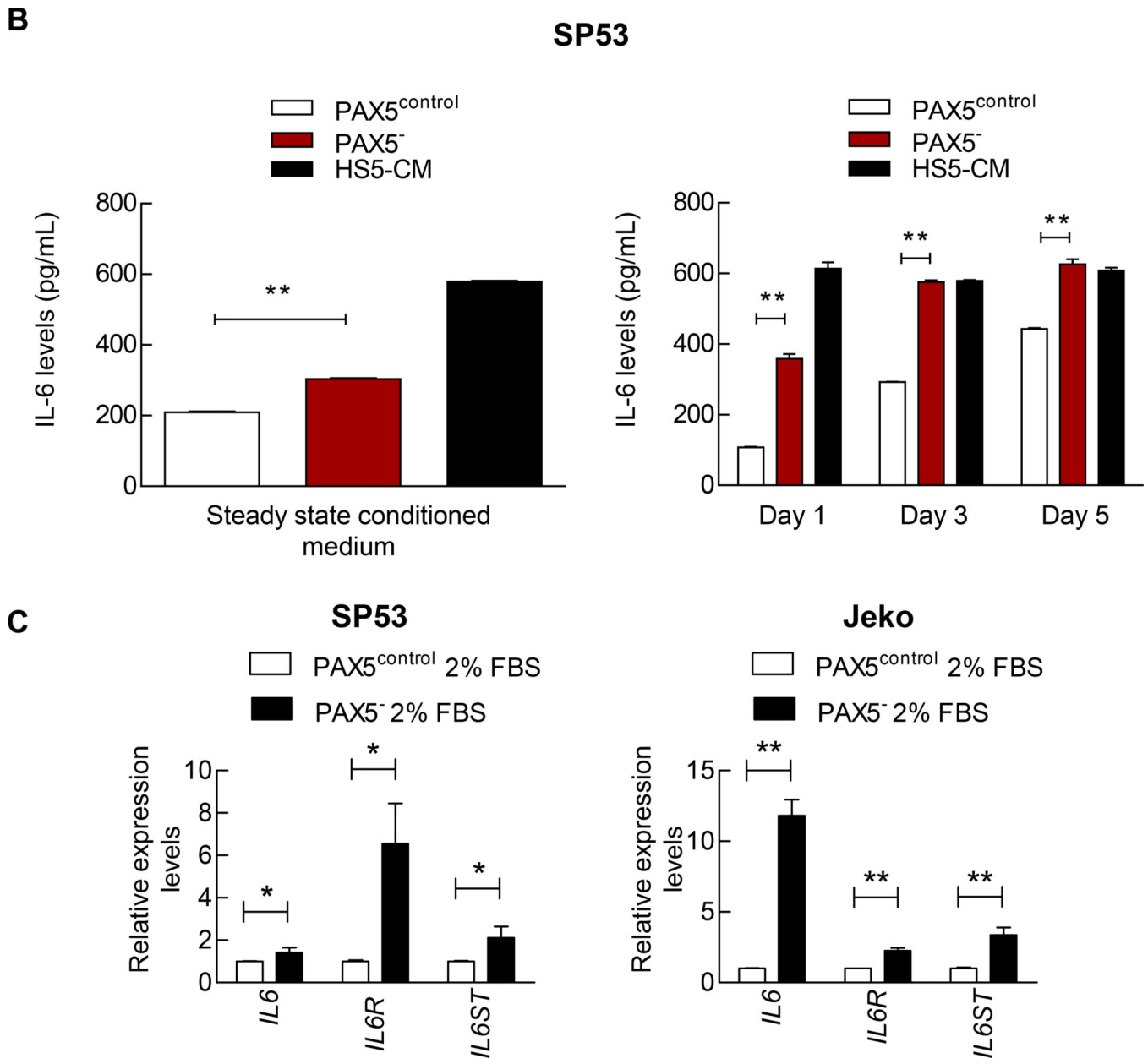

Figure 4b

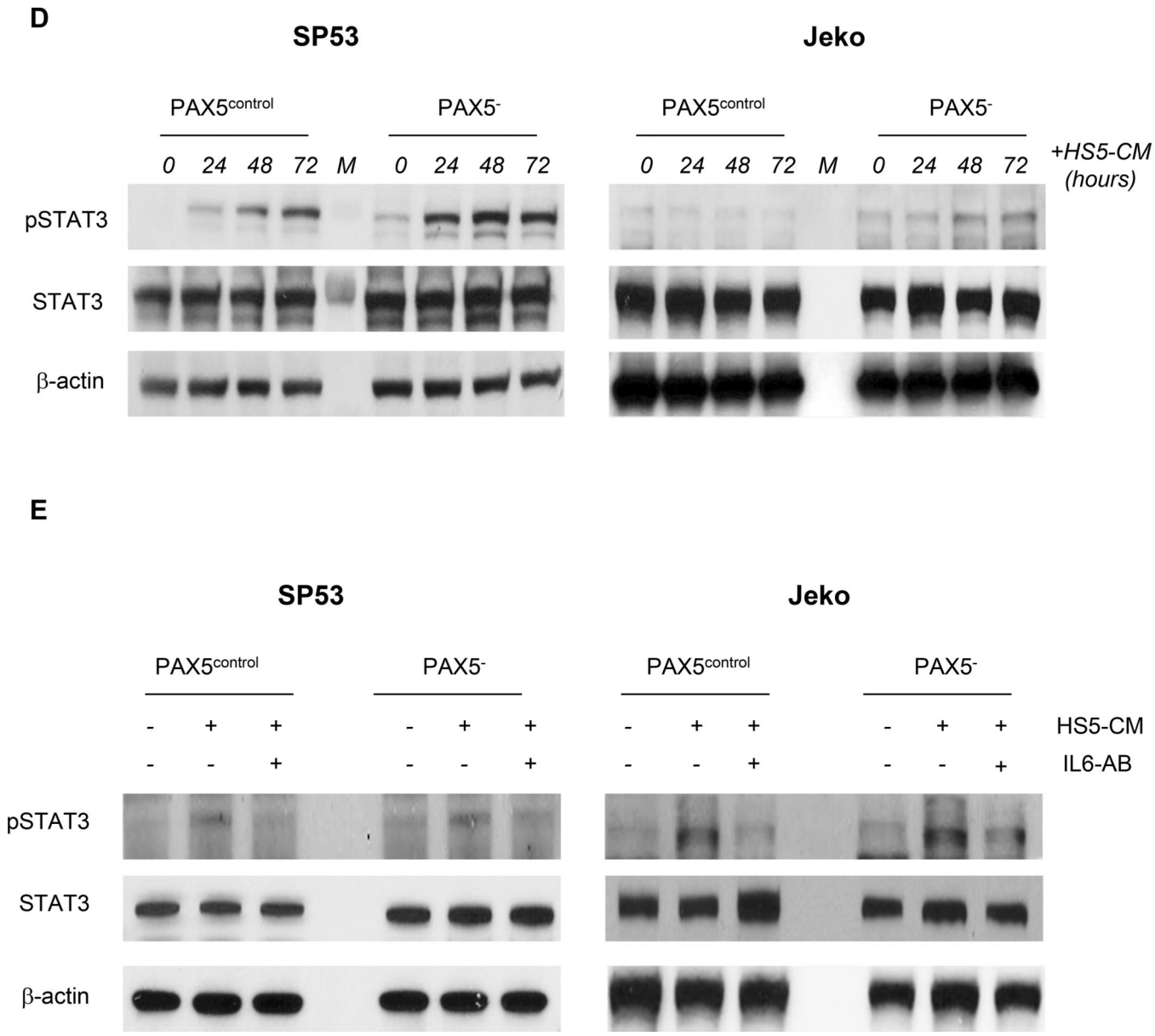

Figure 4c

Figure 4. PAX5⁻ cells overexpress specific pathways involved in cell survival and exhibit increased resistance to bortezomib by facilitating plasmacytic differentiation

(A) Immunoblot analyses of pmTOR, p-p70, p-AKT, pERK, and pMAPK in control and PAX5⁻ MCL cells; β-actin served as the loading control.

(B) ELISA of the IL-6 levels using conditioned media from SP53 PAX5⁻ MCL cells or control cells. The IL-6 levels were analyzed at steady state (*Left*) or during serum withdrawal (*Right*). HS5-CM, which are enriched for IL-6, were used as a positive control.

(C) The levels of IL-6 signaling pathway components were quantified via qRT-PCR. Cells were cultured under low serum conditions for 3 days prior to mRNA harvesting, and the relative expression levels were normalized to GAPDH. **(D)** Immunoblot analyses of pSTAT3 expression in PAX5⁻ and control MCL cells upon the addition of HS5-CM during culturing.

HS5-CM were added to the culture for up to 3 days prior to protein harvesting. Total STAT3 and β-actin served as loading controls. **(E)** $PAX5^{-}$ and control MCL cells exhibited increased pSTAT3 signaling upon HS5-CM addition (30 mins), and this alteration was mediated by IL-6. An IL-6 neutralizing antibody (1 μg) was used to neutralize IL-6 activity in 1 mL of HS5-CM.

*$p < 0.05$ (vs. $PAX5^{control}$; Student's *t*-test); **$p < 0.005$ (vs. $PAX5^{control}$; Student's *t*-test).

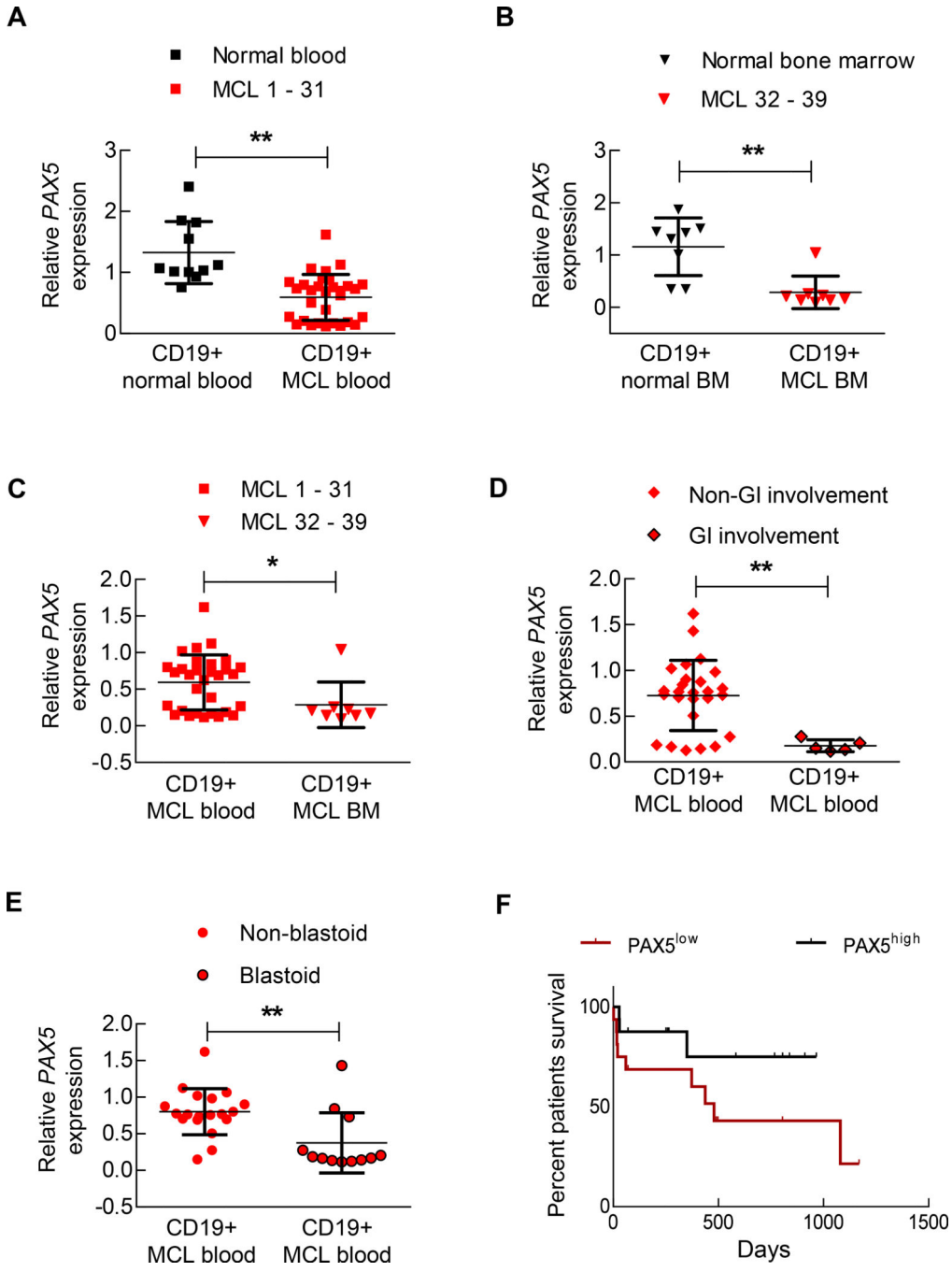

Figure 5. Decreased PAX5 levels in MCL cells promote lymphoma dispersal and can be used to predict a worse prognosis in MCL patients

(A) CD19+ B cells were isolated from MCL biopsy or apharesis samples (n=31) or from normal blood (n=10), and the PAX5 mRNA levels were determined via qRT-PCR. Each replicate was performed in triplicate, and the expression levels were normalized to GAPDH. **(B)** CD19+ cells were purified from bone marrow of normal individuals (n=8) or MCL patients (n=8), and the PAX5 mRNA levels determined via qRT-PCR. Each replicate was performed in triplicate, and the expression levels were normalized to GAPDH. **(C)** PAX5

mRNA was downregulated in the bone marrow samples of MCL patients compared to the corresponding blood samples. **(D)** CD19+ cells isolated from GI-involved MCL patients (n=5) contained lower levels of PAX5 mRNA than CD19+ cells from non-GI-involved MCL patients (n=26). **(E)** CD19+ cells isolated from blastoid MCL patients (n=12) contained lower levels of PAX5 mRNA than CD19+ cells from non-blastoid MCL patients (n=19). A list of samples examined in **(D)** and **(E)** is presented in Supplementary Table 3. **(F)** The overall survival of MCL patients was significantly decreased in the $PAX5^{low}$ population compared to the $PAX5^{high}$ population ($p < 0.05$; Mantel-Cox curve analysis) (n=32). '$PAX5^{high}$' refers to the upper 50% of the PAX5 levels in the MCL patients and '$PAX5^{low}$' refers to who exhibit lower 50% of the PAX5 levels in the MCL patients. A list of samples is presented in Supplementary Table 5. *$p < 0.05$ (vs. $PAX5^{control}$; Student's *t*-test); **$p < 0.005$ (vs. $PAX5^{control}$; Student's *t*-test). n.s. indicates a non-significant difference.

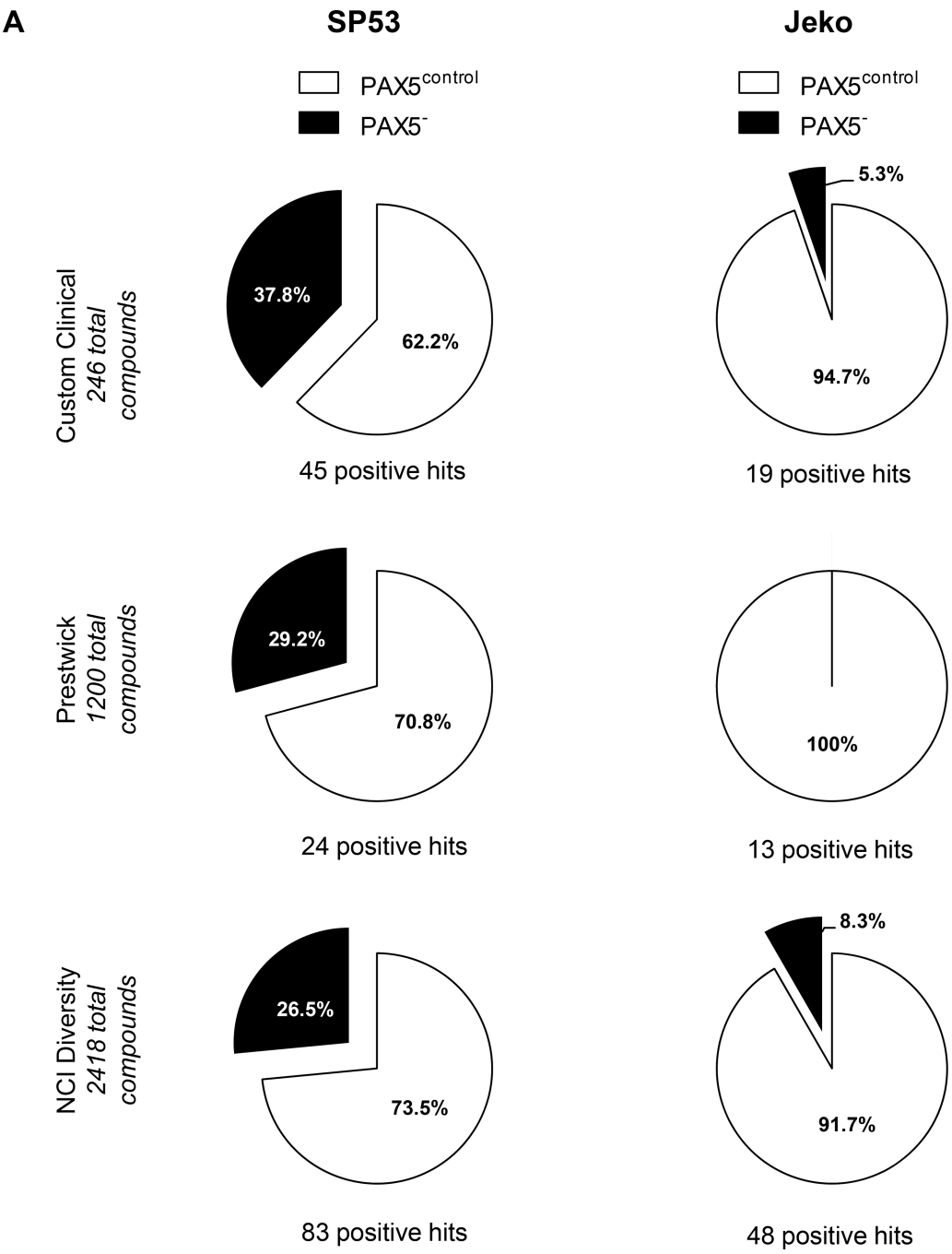

Figure 6a

B

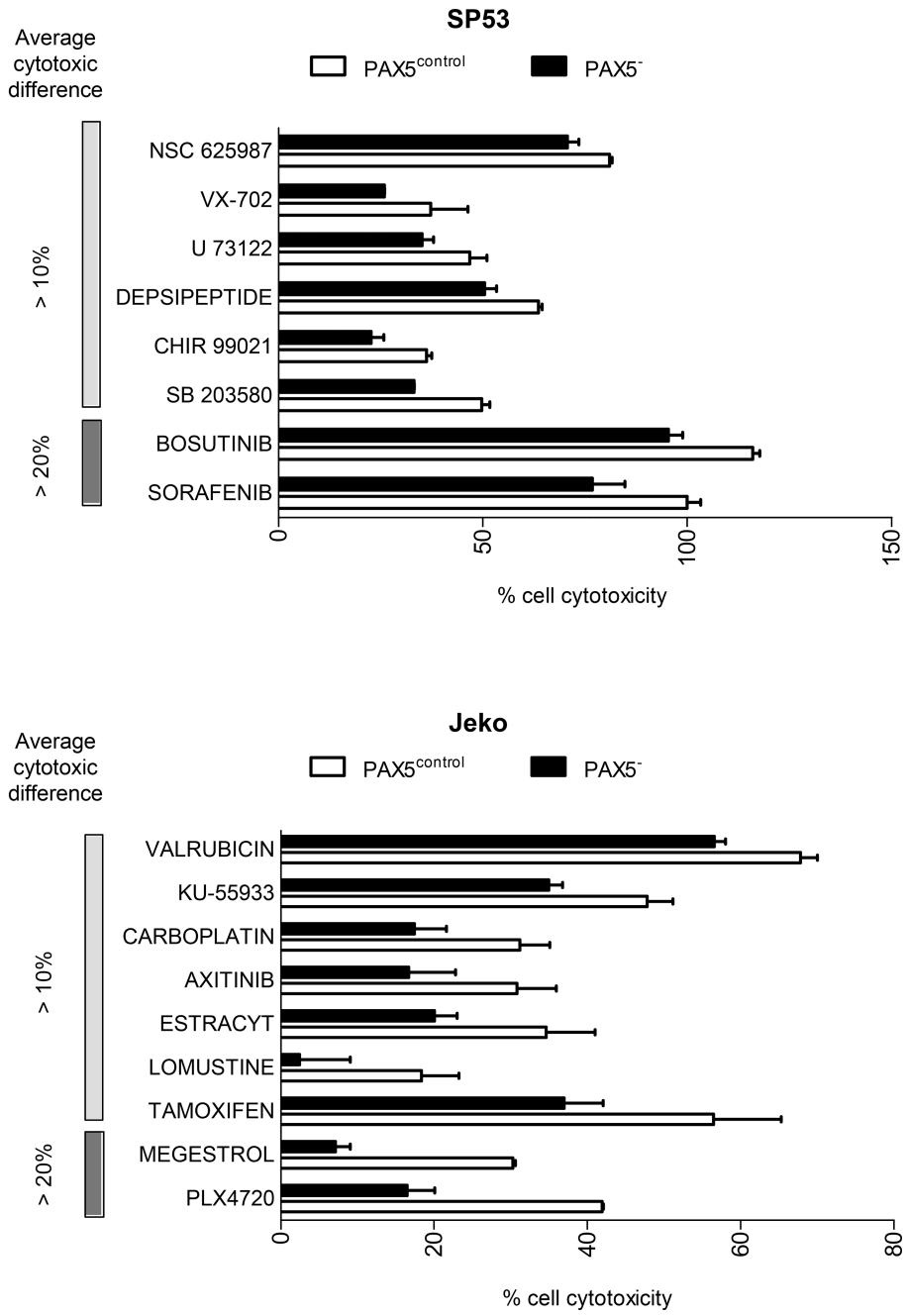

C

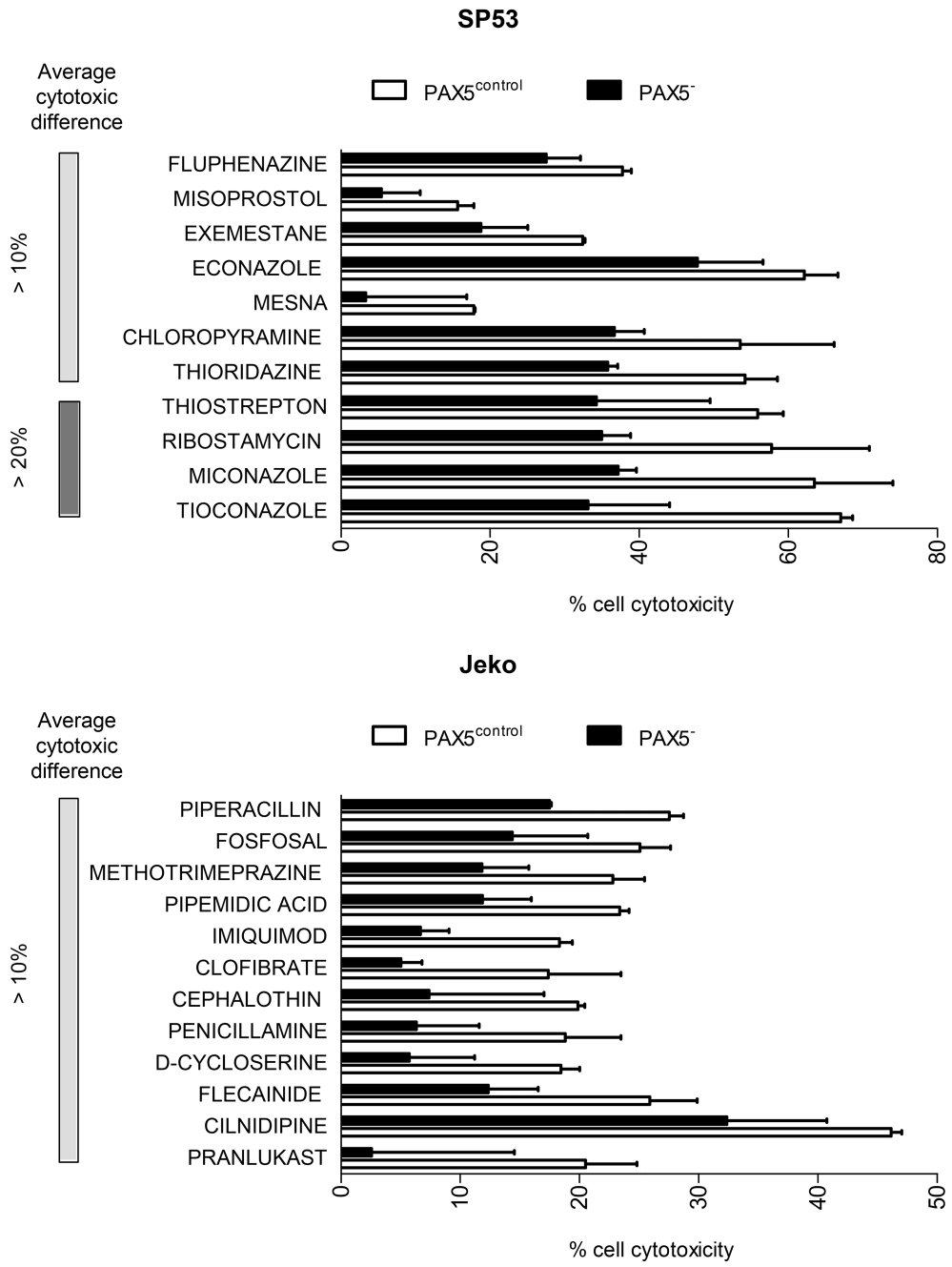

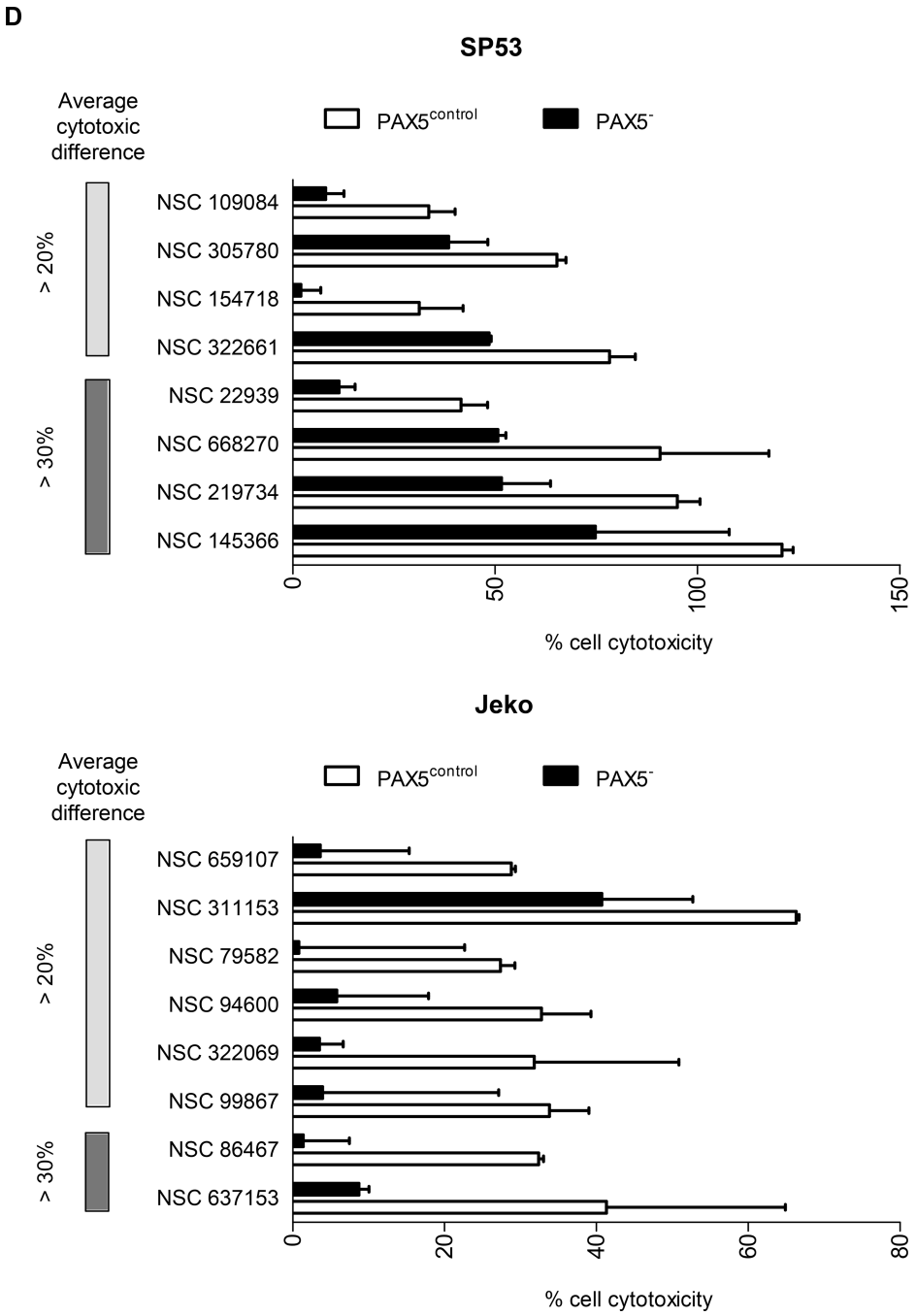

Figure 6b

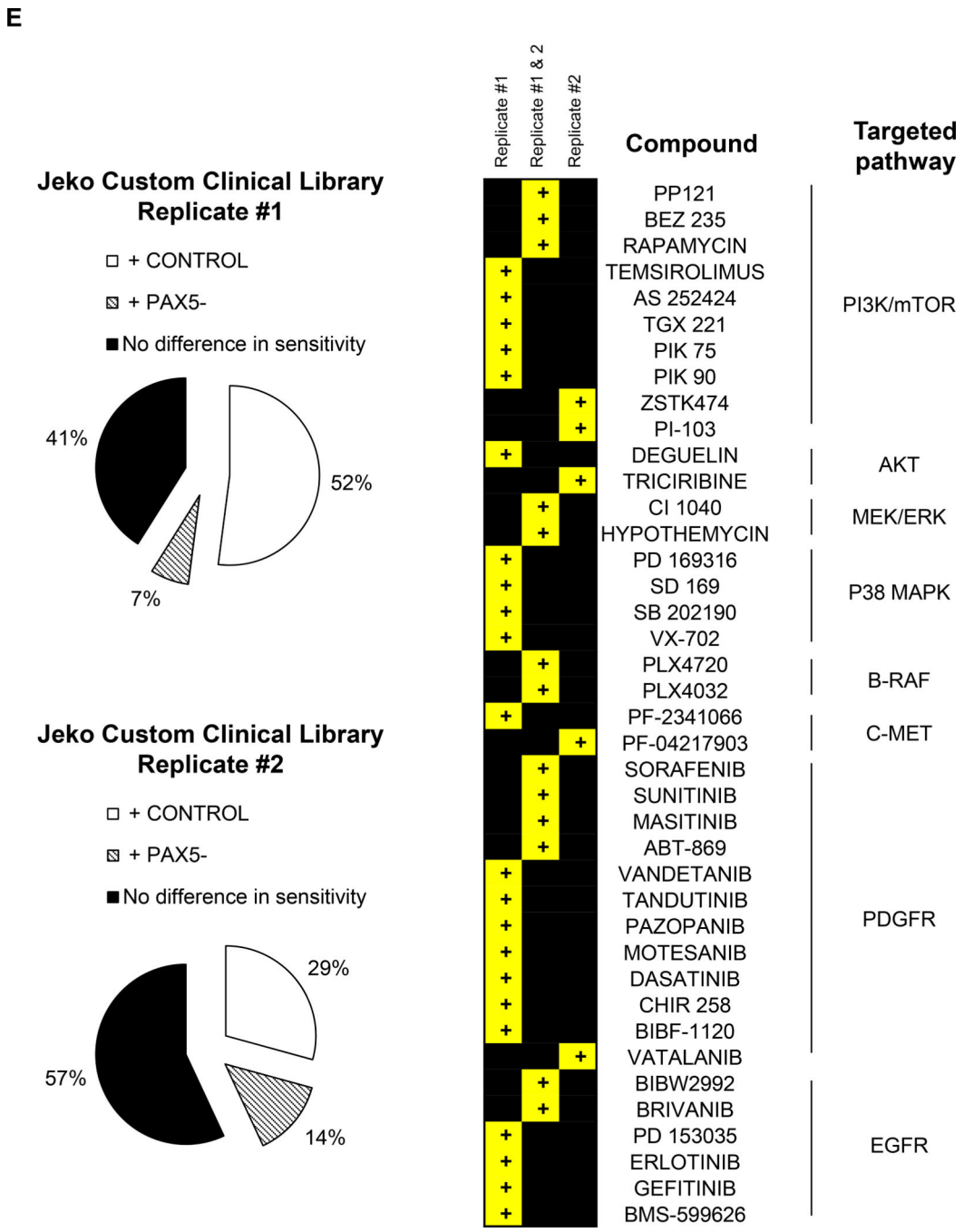

Figure 6e

Figure 6. HTS of compounds reveals the drug-resistant nature of PAX5$^-$ MCL cells

(A) Distribution of compounds examined via HTS that were cytotoxic to each cell type. The proliferation of control cells was inhibited by significantly more compounds than that of PAX5$^-$ cells. Compounds that displayed >40% cytotoxicity were classified as positive hits, and differences between the control and PAX5$^-$ cells (minimum of 5% cell cytotoxicity) were analyzed further. **(B)** A custom clinical library containing compounds with >10% (light gray) and >20% (dark gray) differences in cytotoxicity between the control and PAX5$^-$

MCL cells. **(C)** Prestwick library of compounds with >10% (light gray) and >20% (dark gray) differences in cytotoxicity between the control and PAX5$^-$ MCL cells. **(D)** NCI Diversity library featuring compounds with >20% (light gray) and >30% (dark gray) differences in cytotoxicity between the control and PAX5$^-$ MCL cells. Only compounds that were more cytotoxic to PAX5$^-$ MCL cells were analyzed in **(B), (C)** and **(D)**. **(E)** (*Left*) Jeko PAX5$^-$ cells were more resistant to compounds screened in the Custom Clinical Library (n=2). (*Right*) Inhibitors of the PI3K/mTOR and AKT/MEK/MAPK pathways less strongly induced the cytotoxicity of PAX5$^-$ MCL cells. The array on the right represents compounds targeting components of the aforementioned pathways in two different replicates.

+ CONTROL = Compounds that were more sensitive towards control cells;

+ PAX5$^-$ = Compounds more sensitive towards PAX5$^-$ cells;

+ = compounds more resistant in PAX5$^-$ cells.

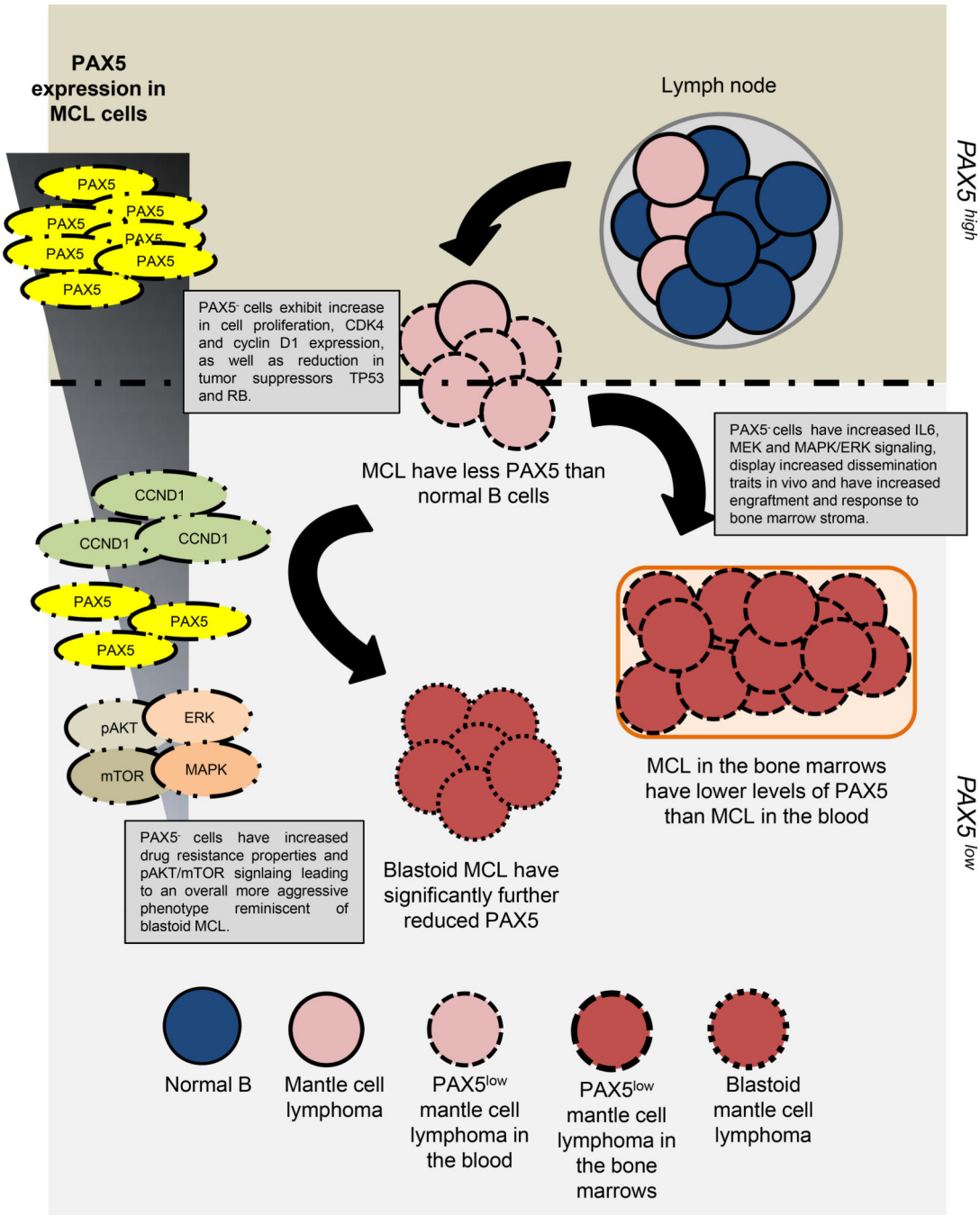

Figure 7. The roles PAX5 signaling in MCL dissemination and prognosis

A model depicting the observations made in this study. MCL patient blood and bone marrow, as well as blastoid MCL samples, displayed significantly lower transcript levels of PAX5. PAX5^{-} Jeko and SP53 MCL cells were generated to emulate this observed PAX5 expression gradient. PAX5^{-} cells exhibited increased proliferation, tumorigenesis, drug resistance, motility and adhesion to the bone marrow microenvironment in vitro and in vivo.

PAX5^{-} MCL cells also exhibited elevated phosphorylation of AKT, mTOR, ERK and p38 MAPK.